Chinese Journal of Chemical Engineering xxx (2017) xxx–xxx

Contents lists available at ScienceDirect

Chinese Journal of Chemical Engineering

journal homepage: www.elsevier.com/locate/CJChE

Review

Recent progress in the green synthesis of rare-earth doped upconversion nanophosphors for optical bioimaging from cells to animals☆

Yuan Pu [1,2], Jingning Leng [1,2], Dan Wang [1,2,*], Jiexin Wang [1,2], Neil R. Foster [2,3], Jianfeng Chen [1,2]

[1] Research Center of the Ministry of Education for High Gravity Engineering and Technology, Beijing University of Chemical Technology, Beijing 100029, China
[2] State Key Laboratory of Organic-Inorganic Composites, Beijing University of Chemical Technology, Beijing 100029, China
[3] Department of Chemical Engineering, Curtin University, Perth, WA 6845, Australia

ARTICLE INFO

Article history:
Received 10 January 2018
Received in revised form 28 February 2018
Accepted 16 March 2018
Available online xxxx

Keywords:
Green synthesis
Upconversion luminescence
Nanomaterials
Biomedical engineering
Imaging

ABSTRACT

Rare-earth doped upconversion nanophosphors (UCNPs), which convert low energy near-infrared (NIR) photons into high energy photons such as ultraviolet, visible light and NIR light, have found various applications in optical bioimaging. In this review article, we summarize recent advances in the synthesis and applications of UCNPs achieved by us and other groups in the past few years. The approaches for the synthesis of UCNPs are presented, with an emphasis on the role of green chemistry in the advancement of this field, followed by a focused overview on their latest applications in optical bioimaging from subcellular structures through cells to living animals. Challenges and opportunities for the use of UCNPs in biomedical diagnosis and therapy are discussed.

1. Introduction

Optical bioimaging uses an optical contrast such as a difference in light transmission, reflection, and photoluminescence (PL) between the region to be imaged and the surrounding region [1,2]. PL based bioimaging is among the most widely used techniques for optical bioimaging, which can be used to visualize morphological details for bio-species, ranging from living cells to animals [3–7]. Compared with other imaging techniques such as ultrasonic imaging, X-ray computed tomography (X-Ray CT), positron emission tomography (PET), single-photon emission computed tomography (SPECT) and magnetic resonance imaging (MRI), PL imaging has the advantage of providing a high signal-to-noise ratio, which enables us to distinguish spatial distributions of even low concentration species and exhibits no harmful radioactivity [8]. For PL bioimaging, labeling of the biological structure with exogenous fluorophores is usually needed since there are many biological structures and processes which cannot be imaged or probed by using intrinsic luminescence [9]. The most commonly used exogenous fluorophores are organic molecules in the past century, though they are suffered from some drawbacks, such as broad emission width and poor photostability, which limit their applications for multiplexed and long-term fluorescent imaging [10–14]. The development of nanotechnology has opened up new frontiers in material science and engineering [15–17] and the luminescent nanomaterials that came with it such as semiconductor quantum dots [18,19], organic-dye doped nanoparticles [20–22], and fluorescent carbon nanodots [23–25], have found many applications in biomedical fields. Most of these conventional luminescent nanomaterials for bioimaging are based on the Stokes-shifted emission with excitation in the ultraviolet (UV) or blue-green visible spectral ranges [18–26], which are limited by at least two disadvantages, namely low signal-to-noise ratio (SNR) due to the autofluorescence from the biological samples when excited at high energy light; and low penetration depth of excitation light and/or emission light in tissues especially for animal imaging [27,28].

Upconversion luminescence refers to a series of nonlinear optical processes that convert two or more lower-energy pump photons, usually near-infrared (NIR) light, to one higher-energy output photon (UV, visible light and/or NIR light) [29–33]. Compared with UV/visible light excitation, the use of NIR excitation light for bioimaging allows deeper light penetration, weaker autofluorescence and lower phototoxicity [33]. Multiphoton absorption and high-harmonic generation based on ultrashort pulsed lasers (*e.g.* femtosecond laser) excitation are two general approaches to achieve photon upconversion in organic dyes and QDs for NIR light excited bioimaging [34,35]. However, ultrashort

☆ Supported by the National Key Research and Development Program of China (2016YFA0201701/2016YFA0201700), the Beijing Natural Science Foundation (2182051), the National Natural Science Foundation of China (21622601), the Fundamental Research Funds for the Central Universities of China (BUCTRC201601), and the "111" project of China (B14004).
* Corresponding author at: Research Center of the Ministry of Education for High Gravity Engineering and Technology, Beijing University of Chemical Technology, Beijing 100029, China.
E-mail address: wangdan@mail.buct.edu.cn. (D. Wang).

https://doi.org/10.1016/j.cjche.2018.03.005
1004-9541/

pulsed lasers have the disadvantages of high cost, complex in maintenance and strict working environment requirement [36]. Rare-earth doped upconversion nanophosphors (UCNPs), by contrast, can realize photon upconversion of continuous wave (CW) NIR light, through the use of long lifetime and real ladder-like energy levels of trivalent lanthanide ions [29–33,36,37]. The photon upconversion emission in UCNPs is attributed to the transitions between physically existing states, which is different from nonlinear multiphoton absorption or high-harmonic generation involving the simultaneous absorption of two or more photons through virtual states [35]. Therefore, the efficiency of photon upconversion process based on UCNPs is much higher than that of nonlinear multiphoton absorption and can perform using a low cost CW NIR laser rather than the use of ultrashort pulsed lasers [37]. In addition to the unique photon upconversion properties, UCNPs show a sharp emission bandwidth, long lifetime, tunable emission, high photostability, and low cytotoxicity, which render them particularly useful for bioimaging applications including cell tracking, tumor targeting and vascular imaging [38–42]. Recently, these UCNPs were shown to act as efficient probes for super-resolution nanoscopy [43,44]. Along with others, we have also demonstrated the potential bio-related applications of UCNPs in optical liquid marbles [30], photodynamic therapy [45–48] and optogenetics [33,49–52]. Although tremendous progress has been achieved and several review articles focusing on the physical properties, synthetic strategies and applications of UCNPs have been provided in the past years [53–57], the "chemical engineering part" of the UCNPs story has only just begun. The development of robust mass-scale UCNPs synthesis methods is one of the key materials challenges and the dialogue between chemical engineers and other researchers (chemists, physicists, and biologists) is necessary.

In this perspective review, we present the significant advances achieved by us and other groups in the past few years on the design, synthesis and applications of rare-earth doped UCNPs. The approaches for the synthesis of UCNPs are presented, with an emphasis on the role of green chemistry (green solvents, novel reactors and process intensification technologies) in the advancement of this field. The promise of UCNPs for optical bioimaging in both cells and animals is systematically discussed. Some challenges and opportunities for the use of UCNPs in biomedical diagnosis and therapy will be put forward based on our own understanding of this field.

2. Materials Synthesis

UCNPs are kinds of guest-host systems where trivalent lanthanide ions are dispersed as a guest in a host lattice with at least one dimension being less than 100 nm [29]. Desirable host materials should have low lattice phonon energies to minimize non-radiative losses and adequate transparency within the wavelength range of interest [58]. Various kinds of host materials have been developed, which can be mainly classified into fluorides ($NaYF_4$, $NaYbF_4$, $NaGdF_4$, LaF_3, GdF_3, *etc.*) and oxides (Gd_2O_3, Y_2O_3, La_2O_3, Lu_2O_3, *etc.*) [59]. Ideal host materials need to have close lattice matches to rare-earth dopant ions for achieving high doping levels [29,59]. In these regards, $NaYF_4$ has been the most popular host materials due to its low phonon energy and high chemical stability [30,60]. The doped lanthanide ions in UCNPs can be either activators that emit the radiation or sensitizers that absorb the excitation irradiation and transfer the absorbed energy to the activators. By selecting various kinds of lanthanide dopants, the UCNPs can show emission in a wide range of light from UV through visible (blue, green, red) to NIR (Fig. 1) [61]. Rare-earth ions such as Er^{3+}, Ho^{3+}, and Tm^{3+} have been well suited for the photon upconversion due to their equally spaced energy levels that facilitate photon absorption and energy transfer steps involved in upconversion processes. Yb^{3+} with a larger absorption cross-section in the NIR region is usually doped as a sensitizer in combination with the activators to enhance the upconversion efficiency.

To date, a variety of methods have been developed for the synthesis of rare-earth doped UCNPs, including but not limited to thermal decomposition, co-precipitation, and hydrothermal synthesis [62–64]. Considerable effort has been devoted to prepare highly crystalline structures for highly efficient upconversion emission [65]. Suitable size and uniform shape of the nanocrystals are the primary prerequisites for bioimaging, in particularly for targeted *in vivo* imaging in animals. The nanoparticles generally have delayed clearance and are mostly excreted through the liver without significant metabolism [66,67], unless they can be made small enough to be excreted *via* the kidney [68]. In another hand, the upconversion luminescence efficiency is of critical importance to improve the SNR of the imaging. In most cases, the upconversion luminescence efficiency can be enhanced by increasing the size of UCNPs, since larger UCNPs mean lower surface area and less surface defects for the non-radiative decay which disturbs the upconversion luminescence.

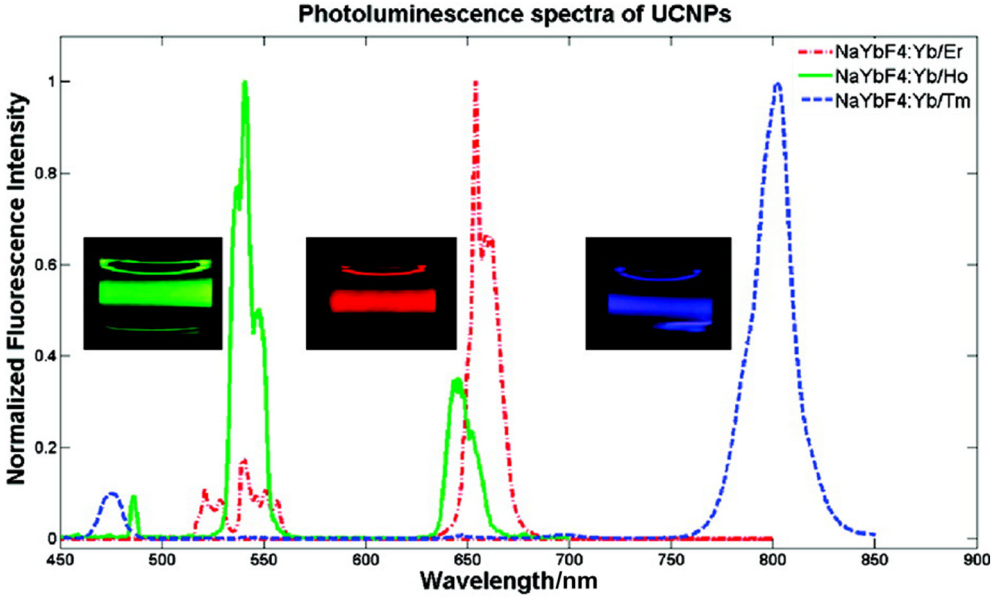

Fig. 1. Upconversion luminescence spectra of Er^{3+}, Ho^{3+} and Tm^{3+} doped UCNPs with red, green and blue emission, respectively. The insets show the visible photoluminescence imaging of the UCNPs colloidal suspension excited by a NIR laser.
Reproduced from Ref. [61] with permission from The American Chemical Society.

Please cite this article as: Y. Pu, *et al.*, Recent progress in the green synthesis of rare-earth doped upconversion nanophosphors for optical bioimaging from cells to animals, *Chin. J. Chem. Eng.* (2017), https://doi.org/10.1016/j.cjche.2018.03.005

Coating of an inert crystalline shell around each particle or employing organic dyes as antennae have also proven to be effective ways to improve the upconversion efficiency of UCNPs, which will be described in the subsequent section [69–73]. In as word, the synthesis of UCNPs with desirable sizes that are large enough to take the advantage of the unique features of the particles (*e.g.* quantum yield) while minimizing the toxicity by using particles small enough to be excreted *via* the urinary tract is a major challenge [74]. To date, considerable efforts have been devoted to exploring the efficiency of various approaches for preparing UCNPs with tunable sizes from sub-10 nm to sub-μm [37]. This section does not aim to give a systematic list of all the synthetic approaches of UCNPs reported. The interested readers are referred to specialized review articles for comprehensive knowledge of UCNPs synthesis [32,37,53,54,56,58,59,65,75–77]. Here we show several selected examples mainly with references to green and scalable preparation of UCNPs based on green solvents, novel reactors and process intensification technologies, to highlight the research area on which already various studies are present, but which should be further intensified.

The thermal decomposition method has been a common route to synthesis high quality UCNPs with highly crystalline phase and narrow size distribution [78]. For the typical synthesis of Yb^{3+} and Er^{3+} co-doped $NaYF_4$ UCNPs through the thermal decomposition method, metallic trifluoroacetate precursors are heated over 300 °C in the presence of surfactants and high boiling organic solvents. The rapid decomposition of metallic trifluoroacetate at high temperature yields monomers, which are then crystallized and grow into monodispersed UCNPs. The oleic acid and/or oleylamine were usually chosen as surfactants to prevent nanoparticle aggregation and the most commonly used organic solvent was octadecene (ODE) due to its high boiling point. The thermal decomposition method has been extended to synthesize several types of monodisperse UCNPs with narrow size distribution, good crystallinity, and desirable optical properties [79]. However, there are two limitations for this approach, including the relatively hash reaction conditions and generation of toxic byproducts of fluorinated and oxyfluorinated carbon species during the pyrolysis of trifluoroacetates (Fig. 2) [80], which make the thermal decomposition method unpractical for the large-scale synthesis of UCNPs. Recently, we have reported the replacement of commonly used ODE with paraffin liquid as the high boiling non-coordinating solvent for thermal decomposition synthesis of $NaYF_4$:Gd^{3+},Yb^{3+},Er^{3+} nanophosphors[35] and $NaYF_4$:Yb^{3+},Tm^{3+} microphosphors [80]. Since paraffin liquid is a more environmentally friendly and much cheaper chemical than ODE [15], the modified method is useful for the development of greener thermal decomposition route for scalable preparation of UCNPs.

Co-precipitation is one of the most promising techniques for large-scale production of nanoparticles [81–83]. In contrast to thermal decomposition method, the co-precipitation synthesis of UCNPs does not need hash reaction conditions or complex procedures and the reactions can be completed in aqueous solutions rather than in organic chemical [84]. For instance, in a typical route for the synthesis of $NaYF_4$:Yb^{3+}, Er^{3+} UCNPs, the particles formed by co-precipitation of the rare-earth chlorides with NaF in the presence of ethylenediamine tetraacetic acid (EDTA), showing spherical shapes with narrow size distribution of 32–46 nm in diameter [85]. Spherical Gd_2O_3:Yb^{3+},Er^{3+} UCNPs can be prepared *via* a simple homogenous co-precipitation of rare earth nitrates with urea in aqueous solution and the particle sizes of were controllable by adjusting the molar ratios of rare earth ions and urea [86]. The co-precipitation method has proven to be a convenient method for the preparation of UCNPs, despite the fact that UCNPs synthesized *via* the co-precipitation process usually require additional post-heat treatment or annealing at high temperatures to sharpen the crystal structure or prompt the phase transfer to obtain products with high upconversion efficiency [87]. During the co-precipitation process, rapid mass transfer and micromixing are critical for the formation of nanoparticles with narrow size distribution [88]. However, the efficiency of mass transfer and micromixing of liquids in traditional stirred tank reactors are limited, and these problems will become more prominent in the case of large-scale production [89]. As one of the cutting-edge process intensification, the high-gravity (Higee) technology based on rotating packed bed reactor has been used to produce various kinds of nanoparticles [83,90]. In particular, we have recently demonstrated the successfully synthesis of Gd_2O_3:Yb^{3+},Er^{3+} UCNPs by Higee reactive precipitation along with a post hydrothermal and calcination process (Fig. 3) [91]. Due to the intensified mixing by the rotating packed bed reactor, the obtained Gd_2O_3:Yb^{3+},Er^{3+} UCNPs exhibited much smaller particle sizes (<100 nm) than that from the common route (~360 nm).

Hydrothermal synthesis of UCNPs involves the mixing of appropriate reaction precursors, solvents and surfactants and then heating of the mixture in a specialized reaction vessel typically known as Teflon-lined stainless steel autoclave [92–94]. The most representative example of hydrothermal synthesis is provided by Li *et al.*, who reported on a general liquid–solid-solution (LSS) strategy for the synthesis of monodisperse nanoparticles [95]. In this strategy, the nucleation and growth of UCNPs occur at the liquid–liquid or liquid–solid interface [95]. The nanoparticles precipitate at the bottom of the reaction vessel, and can

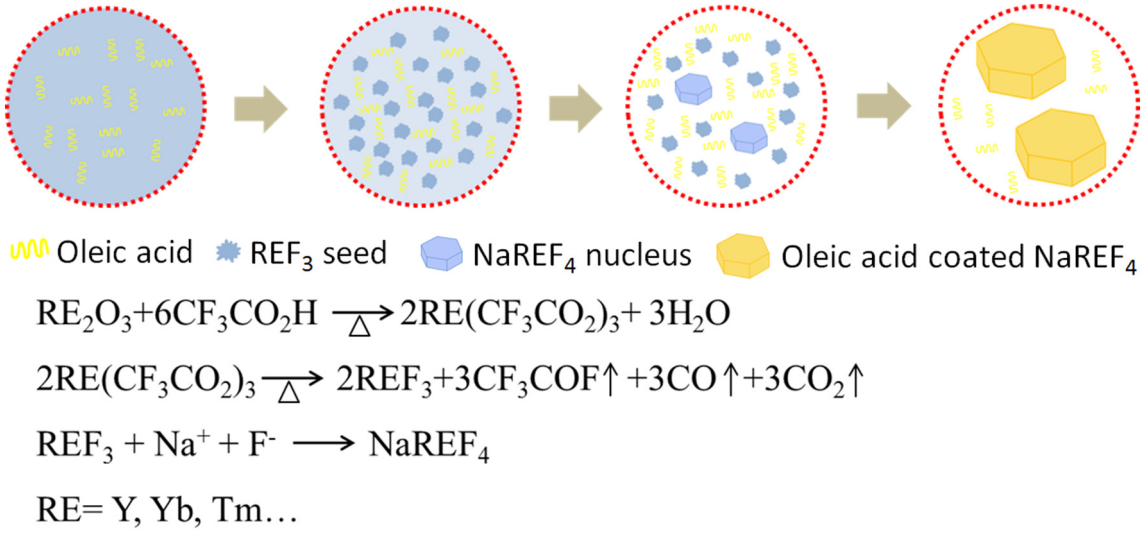

Fig. 2. Schematic diagram of the process and possible chemical reactions involved in the formation of $NaYF_4$:Yb^{3+}, Tm^{3+} particles *via* thermal decomposition approach. Reproduced from Ref. [80] with permission from Elsevier.

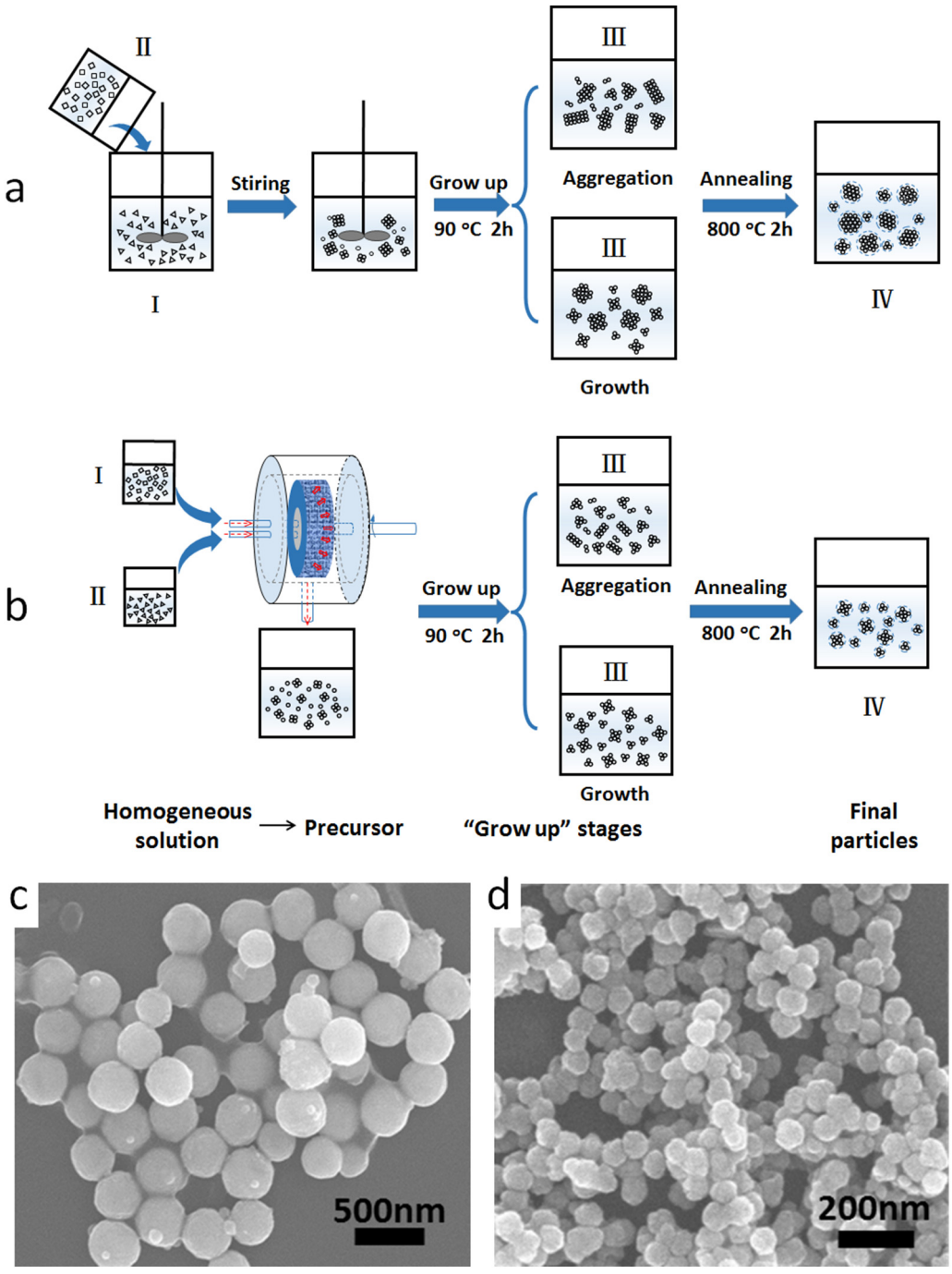

Fig. 3. Schematic diagram of the routes for the preparation of Gd_2O_3:Yb^{3+},Er^{3+} UCNPs without (a) and with (b) Higee process intensification; typical scanning electron microscope (SEM) images of Gd_2O_3:Yb^{3+},Er^{3+} UCNPs obtained without (c) and with (d) Higee process intensification.
Reproduced from Ref. [91] with permission from The American Chemical Society.

be easily recovered and dispersed in nonpolar or moderately polar solvents. The controlled growth of UCNPs of tunable sizes can be theoretically achieved by varying the reaction parameters such as reaction temperature, reaction time and surfactants in the hydrothermal synthesis approach [96–98]. As the reaction conditions are relatively mild, and no particular skills seem to be needed, this method is a prime candidate for large-scale production of UCNPs. However, the stand batch-type reactors do not always allow a fine tuning of conditions, such as fast mixing of the solvents or chemicals, sudden rise or fall of temperatures, when large volumes of solution are involved (*i.e.* in liters or more), leading to low batch-to-batch reproducibility. This is particularly challenging in moving towards UCNPs for large-scale production and commercial applications. An alternative to a batch reactor is continuous reactor [99,100], in which the reactants are continuously fed and the reaction parameters (*e.g.* residence time, temperature and pressure) are better controlled than in batch operations. It is highly recommended to use continuous-type reactors such as rotating packed bed reactor [101,102], microchannel reactor [103,104], and spinning disk processor [105], to meet the conditions for scalable and stable production of UCNPs, although few literatures have been reported. As a conclusive note to the synthesis of UCNPs in rotating packed bed reactors, we can certainly say that many syntheses of UCNPs, at least at laboratory

Please cite this article as: Y. Pu, *et al.*, Recent progress in the green synthesis of rare-earth doped upconversion nanophosphors for optical bioimaging from cells to animals, *Chin. J. Chem. Eng.* (2017), https://doi.org/10.1016/j.cjche.2018.03.005

scale, can be carried out with a rotating packed bed reactor and the obtained UCNPs possess higher quality, namely with regular shape, uniform size and narrow distribution [91].

3. Surface Modification

As mentioned in the above section, UCNPs are typically prepared in the presence of capping ligands (*e.g.* oleic acid, oleylamine) to control the particle growth and stabilize the particles against aggregation in solutions, which are generally hydrophobic. In other cases, additional post-heat treatment or annealing are usually needed for the UCNPs obtained *via* the co-precipitation process in order to sharpen the crystal structure or prompt the phase transfer to obtain products with high upconversion efficiency, which result in bare inorganic powders hard to disperse in liquid solution. For biological applications, the UCNPs are required to be well-dispersed in biological buffers, which are usually aqueous solutions. Surface modification refers to the act of modifying the surface of materials by bringing physical, chemical or biological characteristics different from the original ones. To date, a variety of surface modification methods (Fig. 4), including silica coating [106], ligand exchange [107,108], ligand oxidation [109], ligand attraction [110] and layer-by-layer assembly [111,112], have been reported [113,114]. For detailed discussions on the various surface modification approaches to UCNPs, the reader can refer to dedicated reviews [29,75–77,115].

Generally, surface modification of UCNPs not only enables the nanoparticles to be dispersed in aqueous phase, but also provides a platform to integrate biomolecules/drugs for multifunctional applications. For instance, we have recently developed a multifunctional nanoplatform by coating $NaYF_4$:Gd^{3+}, Yb^{3+}, and Er^{3+} UCNPs with biocompatible transferrin (TRF), a serum protein with good biocompatibility and tumor targeting ability [45]. Protoporphyrin IX (PpIX), a clinically approved photodynamic therapy agent, was loaded into the shell layer of the TRF-coated UCNPs (Fig. 5). The final UCNP@TRF-PpIX nanoparticles were demonstrated to be efficient probes for photodynamic therapy with near-infrared irradiation and luminescence bioimaging. It should be noted that the surface modification technique is applicable for preparation of both hydrophilic and hydrophilic UCNPs. We reported the surface coating of UCNPs with polyhedral oligomeric silsesquioxane (POSS) to make the particles highly hydrophobic and describe the preparation of optically and magnetically active bifunctional UCNPs-based liquid marbles as well as their applications as miniature reactors for studying the photodynamic therapy of cancer cells [30].

Apart from the improvement of biocompatibility, the surface modification can also improve the optical properties of UCNPs, which is the foundation for further applying UCNPs to bioimaging and other fields. Coating of an inert crystalline shell around each particle has proven an effective way to improve the upconversion efficiency of UCNPs. Excellent demonstrations have been made in various host materials [69,70].

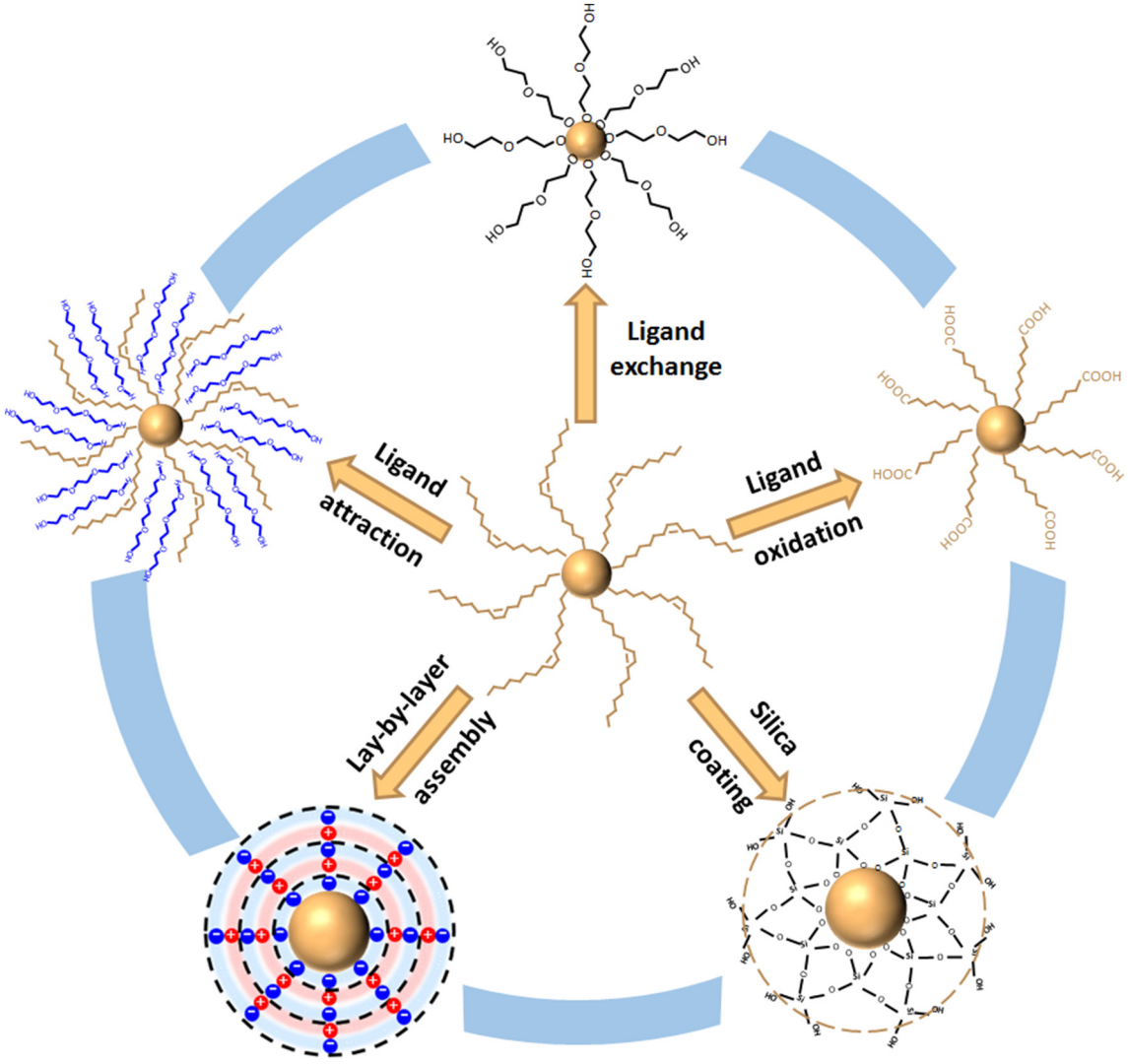

Fig. 4. Schematic illustration of general strategies used for surface modification of UCNPs, including ligand exchange, ligand oxidation, ligand attraction, layer-by-layer assembly, and silica coating.

Please cite this article as: Y. Pu, *et al.*, Recent progress in the green synthesis of rare-earth doped upconversion nanophosphors for optical bioimaging from cells to animals, *Chin. J. Chem. Eng.* (2017), https://doi.org/10.1016/j.cjche.2018.03.005

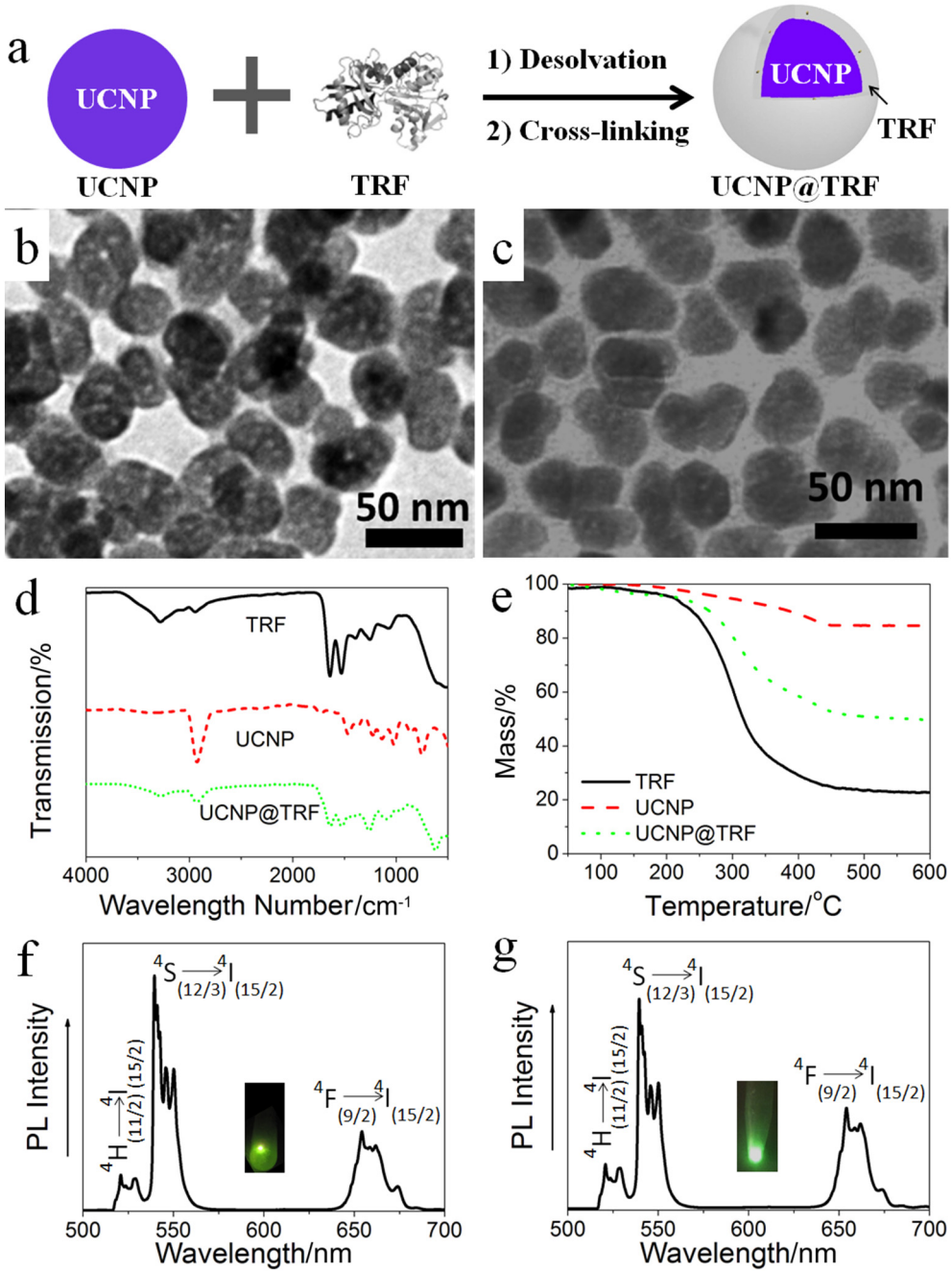

Fig. 5. (a) A schematic illustration of the fabrication of UCNP@TRF nanoparticles; TEM images of (b) UCNP and (c) UCNP@TRF nanoparticles; (d) FTIR spectra and (e) TGA curves of TRF, UCNP and UCNP@TRF nanoparticles, respectively; room temperature upconversion luminescence spectrum of 5 mg UCNPs (f) and UCNP@TRF (g) powder under NIR light excitation with a 980 nm laser at a powder density of 5 W cm^{-2}. Inset: Photographs of the UCNP and UCNP@TRF samples under NIR light excitation, respectively.
Reproduced from Ref. [45] with permission from The Royal Society of Chemistry.

For example, Han and co-workers reported the tunable NIR-to-UV upconversion luminescence enhancement in CaF_2-coated α-$NaYF_4$:Yb^{3+},Tm^{3+} core/shell UCNPs [96]. Optimization of the four-photon UV luminescence in the (α-$NaYF_4$:Yb^{3+},Tm^{3+})/CaF_2 core/shell system yields the maximum quantum yield of 0.1%, which is over 9 times brighter than the known optimal (β-NaYF4:Yb^{3+},Tm^{3+})/β-$NaYF_4$ core/shell UCNPs in aqueous phase [70]. In other examples, employing organic dyes as antennae to enhance the efficiency of UCNPs has emerged as a new dimension [49,71]. Reports have shown that the upconversion luminescence brightness can be increased by a factor of ~3300 for NIR dye sensitized β-$NaYF_4$:Yb^{3+},Er^{3+} nanoparticles and by up to 100 times for NIR dye sensitized ($NaYbF_4$:Tm^{3+})/($NaYF_4$:Nd^{3+}) core/shell, compared with original ones [72,73].

4. *In vitro* Optical Imaging of Cells

The upconversion luminescence is the most fascinating feature of UCNPs that makes them attractive for bioimaging. Compared with the traditional luminescence nanomaterials, the UCNPs possessing spectrally narrow and tunable emission bands excitable by a single wavelength in NIR, can be readily employed as probes for multiplexed bioimaging [116]. In addition, as a typical upconversion luminescence imaging system shown in Fig. 6a [45], the imaging background produced by the scattering or autofluorescence of biological samples from the excitation light can be reduced by using short-pass filters. Thus the anti-Stokes character of the upconversion emission excludes the background signals, resulting in a high signal-to-noise ratio [117].

Please cite this article as: Y. Pu, *et al.*, Recent progress in the green synthesis of rare-earth doped upconversion nanophosphors for optical bioimaging from cells to animals, *Chin. J. Chem. Eng.* (2017), https://doi.org/10.1016/j.cjche.2018.03.005

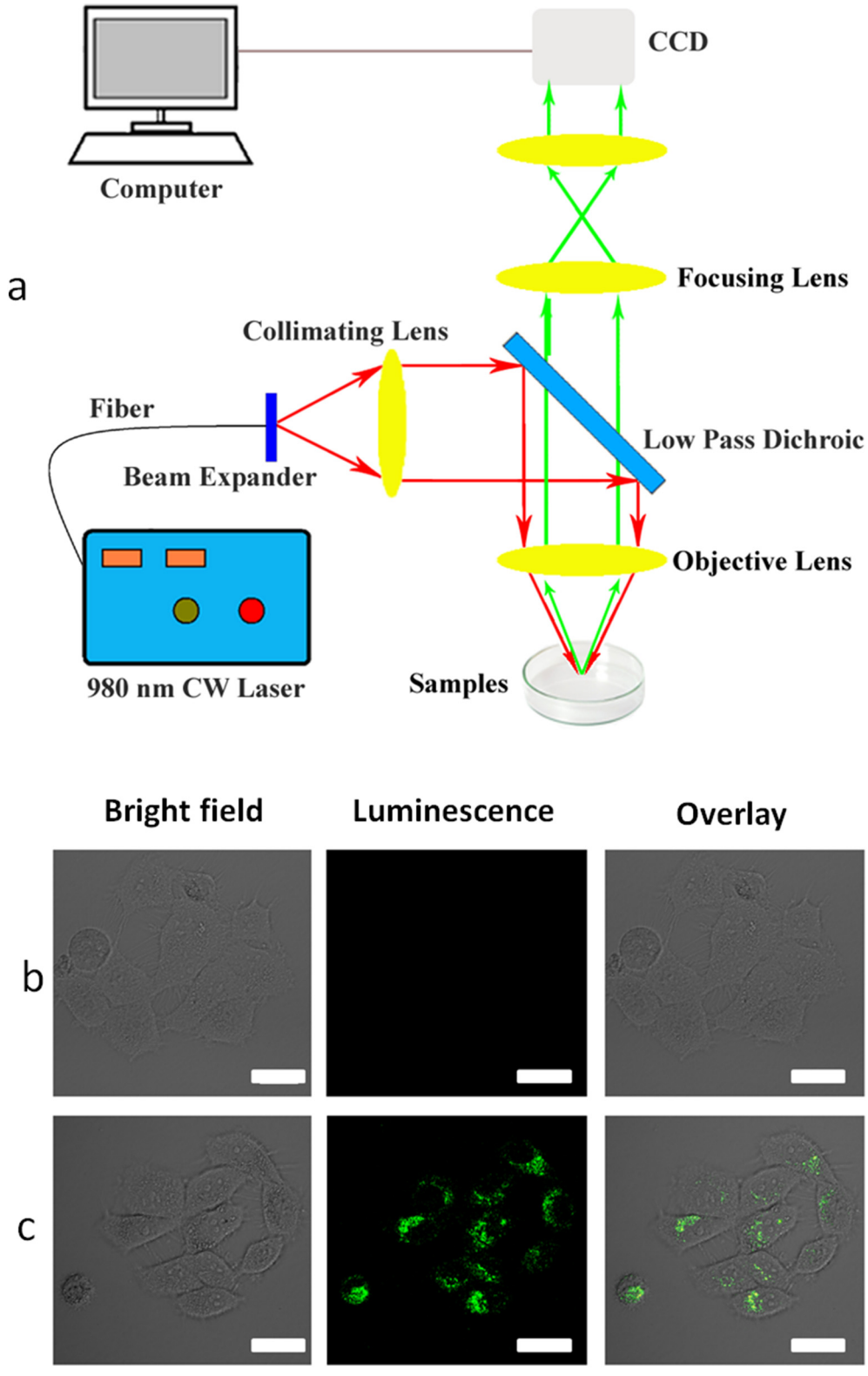

Fig. 6. (a) A typical Upconversion luminescence imaging system; *in vitro* upconversion luminescence imaging of MDA-MB-231 cancer cells incubated in 2 ml of DMEM culture media with the addition of (b) nothing and (c) 200 μl aqueous dispersion of transferrin-coated $NaYF_4$:Gd^{3+},Yb^{3+},Er^{3+} UCNPs (20 $\mu g \cdot ml^{-1}$) for 2 h at 37 °C. The scale bars represent 50 μm. Reproduced from Ref. [45] with permission from The Royal Society of Chemistry.

Zijlmans and co-workers were the first to use the upconversion luminescence of UCNPs for cellular imaging in 1999 [118]. Since then, considerable research efforts have been dedicated to exploit UCNPs as fluorescent probes for *in vitro* imaging of cells, which exhibited significantly low background autofluorescence [39–45,119–122]. Li *et al.* developed a three-dimensional visualization method of laser scanning up-conversion luminescence microscopy with little photobleaching and no background fluorescence by introducing a reverse excitation dichroic mirror and the confocal pinhole technique, obtaining the first quantitative data for the lack of autofluorescence under 980 nm

Please cite this article as: Y. Pu, *et al.*, Recent progress in the green synthesis of rare-earth doped upconversion nanophosphors for optical bioimaging from cells to animals, *Chin. J. Chem. Eng.* (2017), https://doi.org/10.1016/j.cjche.2018.03.005

excitation [121]. Zhan *et al.* proposed a multi-photon evanescent wave (EW) excitation modality for UCNP-based microscopy and the particles tracking and *in vitro* cell membrane imaging were performed with ultrahigh contrast and high spatiotemporal resolution [122]. Our group demonstrated the efficient uptake of transferrin-coated magnetic UCNPs by MDA-MB-231 cancer cells using upconversion luminescence imaging (Fig. 6b), which has instructional significance for further drug delivery studies based on the nanoplatform of UCNPs [45].

Due to the fact that the sensitizer ion Yb^{3+} has a high absorption cross-section in its absorption band, a low-cost commercial CW laser diode with peak wavelength of 980 nm is usually used to excite the UCNPs for upconversion luminescence in bioimaging due to the fact that the sensitizer ion Yb^{3+} has a high absorption cross-section in its absorption band. However, the high absorbance of 980 nm light by water, results in significant heating effect of a biological tissue under irradiation of 980 nm light [123]. He and co-workers investigated the proposed the use of the 915 nm laser, to excite $Tm^{3+}/Er^{3+}/Ho^{3+}$-doped $NaYbF_4$ UCNPs in the upconversion luminescent bioimaging [61]. The comparison of imaging at 980 nm and 915 nm excitation, along with evaluation of the thermal effect produced by both wavelengths, demonstrated the 915 nm light was better choice (Fig. 7) [61]. Later, Zhong *et al.* reported the use of Nd^{3+}-sensitized UCNPs as luminescent labels for cell imaging, which are excitable at 800 nm due to the incorporation of Nd^{3+} ions into the outer shell [124]. The low water absorption of the 800 nm laser source not only helps to minimize tissue overheating, but can also result in a deep penetration depth for potential *in vivo* imaging [125].

Recently, along with the rapid development on super-resolution optical microscopy, the use of UCNPs for *in vitro* optical imaging has been extended to stimulated emission depletion (STED) microscopy [43,44, 126,127]. Kolesov *et al.* demonstrated the background-free subdiffraction optical microscopy with praseodymium-doped yttrium aluminum garnet (Pr:YAG) UCNPs and achieved all optical resolution of 50 nm [126]. Due to the fact low-efficiency YAG:Pr^{3+} UCNPs emitting toxic UV light under a complicated excitation scheme, their bioimaging applications were limited. Later, using $NaYF_4$:Yb^{3+},Er^{3+} UCNPs, Zhan *et al.* proposed an optical luminescence depletion mechanism and explore their potential for multi-photon STED-like microscopy [127]. Very recently, Liu *et al.* realized low-power super-resolution stimulated emission depletion (STED) microscopy based on high concentration Tm-doped (8%) $NaYF_4$:Yb^{3+}, Tm^{3+} UCNPs, and obtained optical resolution of 28 nm, namely, 1/36 of the wavelength [43]. Zhan and co-workers reported the use of ion-ion interaction to suppress the enhancement effect and enhance the depletion effect of the depletion laser beam, resulting in large optical depletion of upconversion luminescence in a major group of UCNPs. reported the super-resolution imaging of immunostained cytoskeleton structures of fixed cells (resolution ~82 nm) using high Tm^{3+}-doped UCNPs ($NaGdF_4$:18% Yb^{3+},10% Tm^{3+}) as luminescent labels (Fig. 8) were performed [44]. These results demonstrated the ability of UCNPs-mediated super-resolution optical microscopy technique for imaging subcellular structures.

5. *In vivo* Optical Imaging of Animals

In the case of animal imaging, the limitations of fluorescence imaging based on short-wavelength light excitation are more prominent, due to the Rayleigh scattering effect and significant background signal associated with autofluorescence of biological tissues such as fur, skin, and food in the subject studied. Following an intravenous injection of 3-mercaptopropionic acid coated $NaYF_4$:Yb^{3+},Tm^{3+} UCNPs into Balb-c mice, Prasad *et al.* [128] performed *in vivo* whole-body imaging of mice, in which the NIR upconversion luminescence signal of UCNPs peaking at ~800 nm was readily detectable through the skin (without hair removal) of the mice. The obtained high contrast images clearly demonstrate the feasibility to image and spectrally distinguish the characteristically emitting UCNPs. Later, the advantages of upconversion luminescence imaging with UCNPs were revealed in *in vivo* animals [37, 129–134]. For instance, as shown in Fig. 9, Pan *et al.* [134] performed *in vivo* whole-body images of mice injected with silica coated UCNPs with and without folic acid modification. The upconversion luminescence signals were collected through the skin of mice (without hair removal), from which the gastric cancer tissues were identified *in vivo* due to the targeted ability of folic acid conjugated UCNPs to tumors.

As for *in vivo* bioimaging, tremendous progress has been achieved on the development of UCNPs for optical bioimaging in mice using NIR (980 nm)-to-NIR (800 nm) upconversion luminescence [135–137]. However, the optical imaging technique (even for NIR-to-NIR luminescence imaging) is still limited by their relatively low penetration depth in animals (maximum to several centimeters) [37]. There is a growing

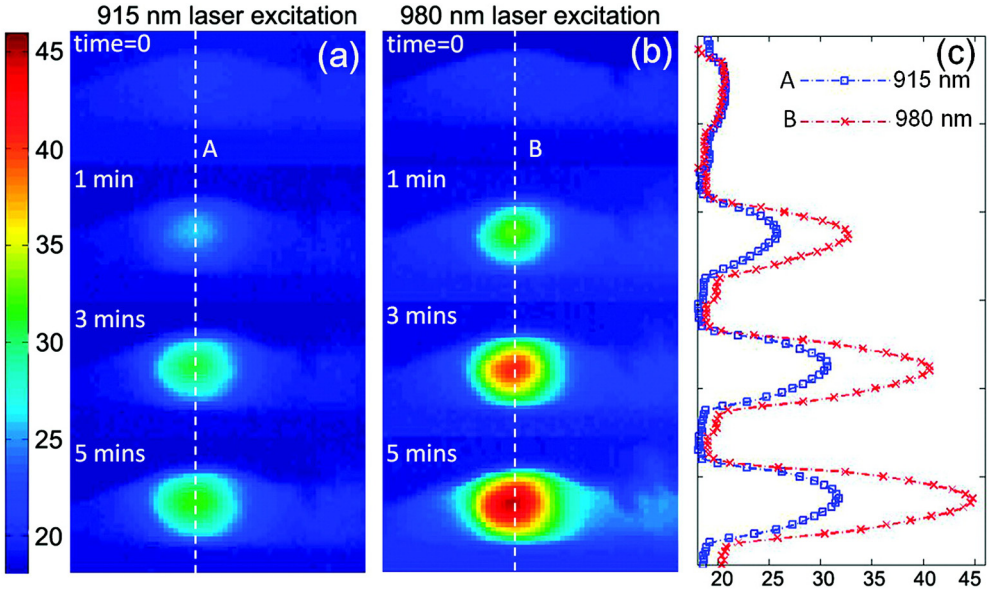

Fig. 7. Experimental temperature (°C) distributions after different irradiation times for (a) 915 nm laser irradiated mouse skin and (b) 980 nm laser irradiated mouse skin and (c) the corresponding temperature line profiles (curves A and B in (c) corresponding to line A in (a) and line B in (b), respectively).
Reproduced from Ref. [61] with permission from The American Chemical Society.

Please cite this article as: Y. Pu, *et al.*, Recent progress in the green synthesis of rare-earth doped upconversion nanophosphors for optical bioimaging from cells to animals, *Chin. J. Chem. Eng.* (2017), https://doi.org/10.1016/j.cjche.2018.03.005

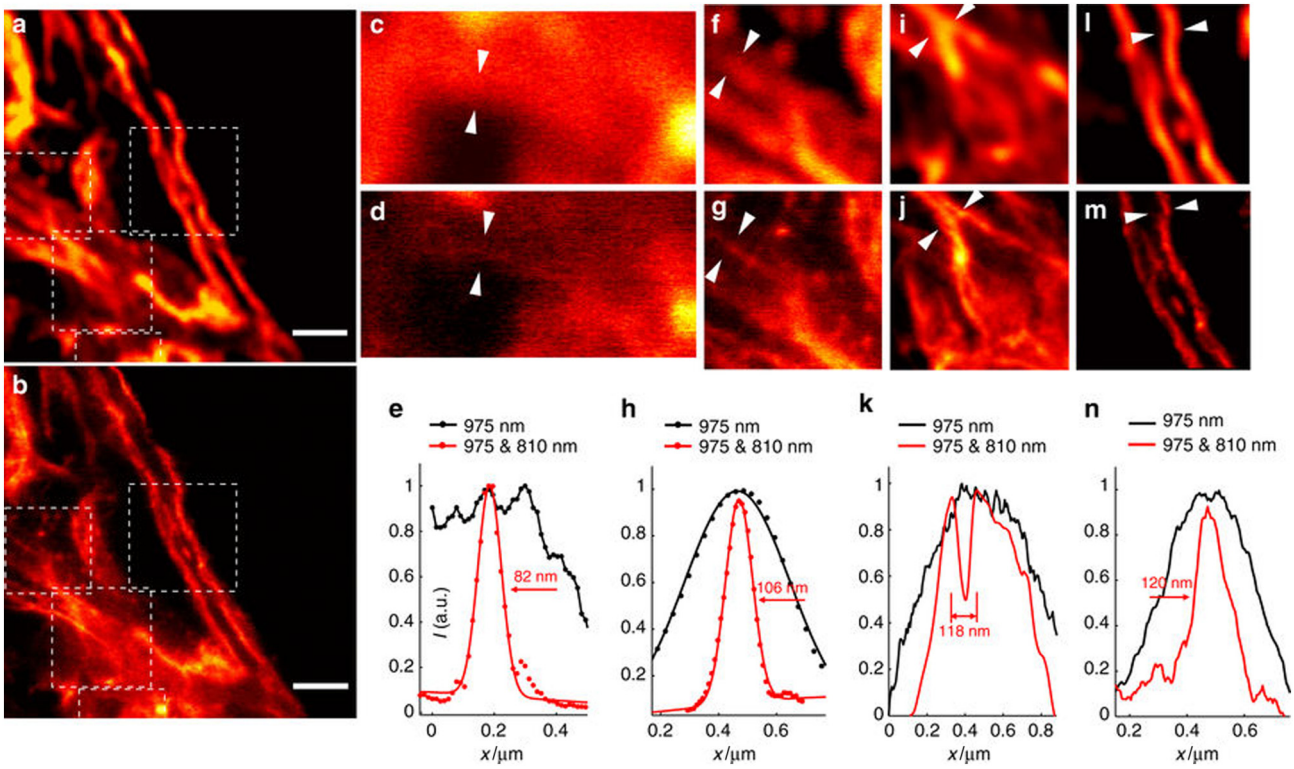

Fig. 8. Immunofluorescence labeling of cellular cytoskeleton protein desmin with antibody-conjugated UCNPs and super-resolution imaging: (a) the multiphoton imaging under 975-nm excitation of some cytoskeleton structures and desmin proteins in HeLa cancer cells incubated with anti-desmin primary antibody and immunostained with UCNPs (11.8 ± 2.2 nm in diameter) bioconjugated with goat anti-rabbit IgG secondary antibody; (b) the same region with a imaged in the super-resolution mode (975-nm excitation and the 810-nm STED laser beam); (c-n) magnified areas selected from (a) and (b) (marked by white dotted squares) and line profile analyses; images in c, f, i, and l are taken from the white dotted squares in a; Images in d, g, j, and m are taken from the white dotted squares in b. e, h, k, n Line profiles analyses of several areas indicated by arrow heads in c and d, f and g, i and j, and l and m, respectively. The scale bars in (a) and (b) represent 2 μm.
Reproduced from Ref. [44] with permission from Springer Nature.

interest in the development of UCNPs that can function as multiple contrast agents for simultaneous use in different medicinal imaging modalities (*e.g.*, X-Ray CT, PET, SPECT, and MRI) to achieve "real" deep imaging [138–140]. In addition to the ability for luminescence diagnosis, UCNPs also hold great potentials to "light-up" the cells in deep tissues for other photoactivation applications such as photodynamic therapy, and optogenetic studies [49–52,141,142]. Since the topic of this review article is focused on the optical bioimaging based on photon upconversion, we will not include detailed discussions on the applications of UCNPs for multimodal imaging, photodynamic therapy and optogenetic studies, which nevertheless should be interesting topics in future directions. It should be mentioned that for *in vivo* upconversion luminescence diagnosis and photodynamic therapy, the UCNPs are usually required to be given by intravenous injection and be small enough (*e.g.* sub-10 nm) for long-time circulation in animals. In contrast, for optogenetics applications, the upconversion phosphors are expected to be embedded at a particular location in the neuronal plasma membrane, where the neurons are controlled by the exogenous expression of light-sensitive ion channels. Upconversion phosphors with large size (*e.g.* a few microns in diameter) and high upconversion efficiency are preferable for applications in optogenetic studies than nanophosphors. Fig. 10 shows a recent work by our group, revealing the *in vivo* upconversion luminescence imaging of mice after microinjection of $NaYF_4$:Yb^{3+},Tm^{3+} microphosphors in the brain tissue of mice. The distribution depth of interested cells such as cerebellum and cerebral cortex in small mice were generally less than 800 μm in their brains and $NaYF_4$:Yb^{3+},Tm^{3+} microphosphors can achieve such a depth for *in situ* light upconversion from near-infrared to blue. Combined with the fact that microphosphors distribution was concentrated in a very small area (500 μm × 500 μm × 50 μm), this make the particles promising for *in vivo* optogenetic studies [80].

6. Summary and Prospect

Photon upconversion based on rare-earth doped UCNPs has tremendous attention in many fields, including bioimaging, anti-counterfeiting, photovoltaic devices, photodynamic therapy, and other photoreactions. In this article, we focus on the recent advances of UCNPs for optical bioimaging achieved by us and other groups in the past few years and present an overview on the synthesis, surface modification and bioimaging of UCNPs. Even this short perspective review article has revealed the versatility of UCNPs for bioimaging, from *in vitro* upconversion luminescence imaging in cells through *in vivo* macroscopic imaging to microscopic imaging in animals. However, the applications of UCNPs for bioimaging are still at its early stage with many important issues remained to be addressed:

(1) Widely applications of the UCNPs will not be realized if there is no facile and large-scale fabrication capability for UCNPs with well-defined properties desirable for applications. We have remarked, however, the scalable synthetic approaches for mass production of UCNPs with tailor-made structures are still limited. This is a direction in which chemical engineers should involve. As an alternative to commonly used batch reactor for UCNPs synthesis, continuous reactors are highly recommended to overcame the limitations of batch reactors and meet the conditions for scalable and stable production of UCNPs.
(2) Like many other nanomaterials for biomedical applications, there are concerns about the possible side effects derived from the use of UCNPs. Although rare-earth doped UCNPs possess no toxic elements and are generally considered as biocompatible materials after surface modification [143],

Please cite this article as: Y. Pu, *et al.*, Recent progress in the green synthesis of rare-earth doped upconversion nanophosphors for optical bioimaging from cells to animals, *Chin. J. Chem. Eng.* (2017), https://doi.org/10.1016/j.cjche.2018.03.005

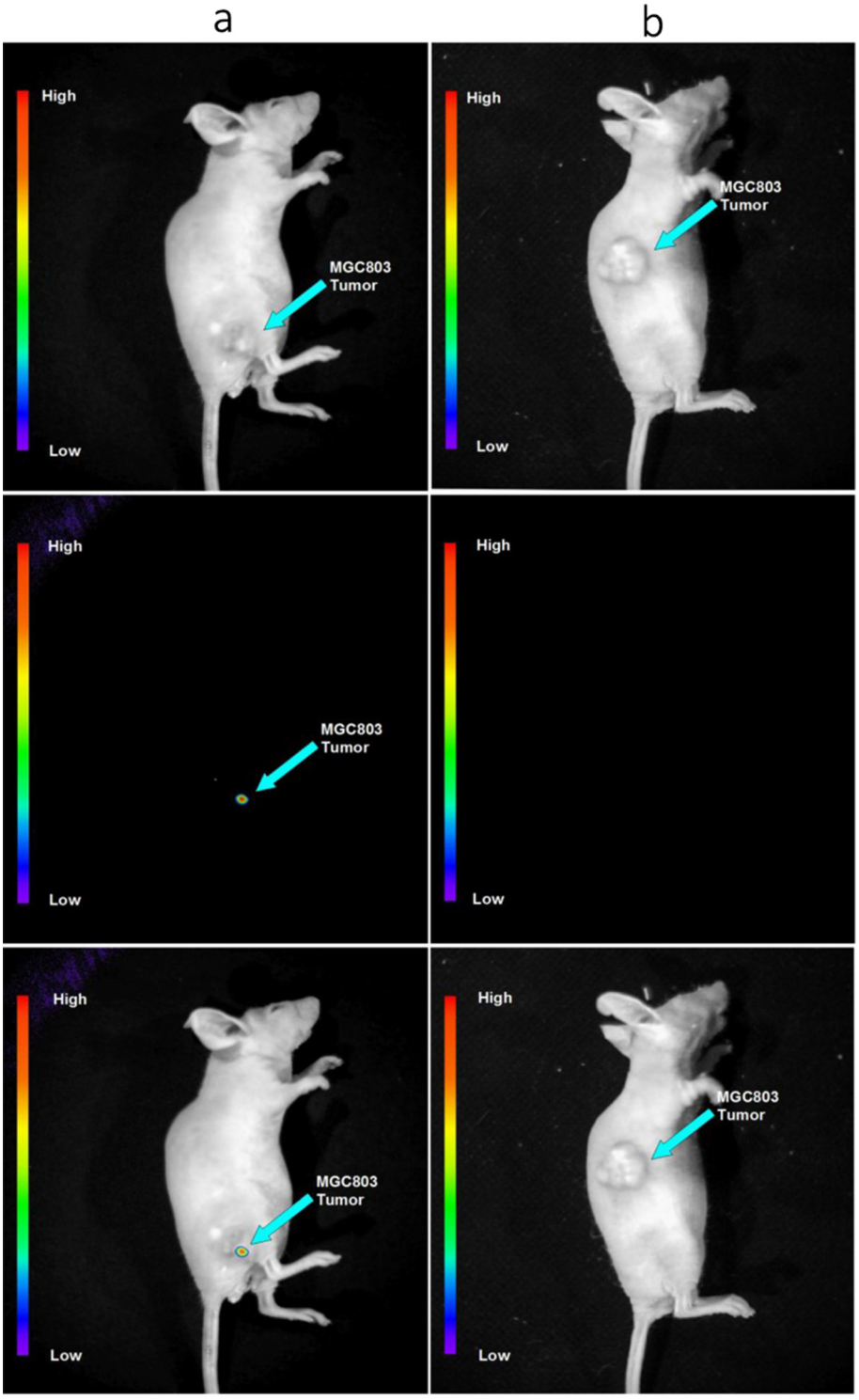

Fig. 9. Targeted *in vivo* NIR upconversion luminescence imaging of subcutaneous MGC803 tumor (indicated by short arrows) after intravenous injection of silica coated $NaYbF_4$:Gd^{3+}, Tm^{3+} UCNPs (a) with and (b) without folic acid modification.
Reproduced from Ref. [134] with permission from Ivyspring International Publisher.

nanotoxicity studies of UCNPs (with different components, sizes, shapes, and surface coatings) to human and other biological systems need to be carefully ascertained. Along with the cytotoxicity researches at the cellular level and histological toxicity investigations in animal level, potential hazards of UCNPs to DNA damage (*i.e.*, genotoxicity) are also important since there is a close correlation between DNA damage and mutation or cancer.

(3) There are already very big improvements on the upconversion efficiency of UCNPs in recent years. The reported upconversion quantum yields of current UCNPs remains rather limited for all *in vivo* optical bioimaging, especially under low irradiance. The integrations of upconversion luminescence imaging with other biomedical imaging techniques such as X-Ray CT, PET, SPECT, and MRI, enable accurate diagnostics in a reduced time frame. Development of multifunctional probes to cover both diagnosis

Please cite this article as: Y. Pu, *et al.*, Recent progress in the green synthesis of rare-earth doped upconversion nanophosphors for optical bioimaging from cells to animals, *Chin. J. Chem. Eng.* (2017), https://doi.org/10.1016/j.cjche.2018.03.005

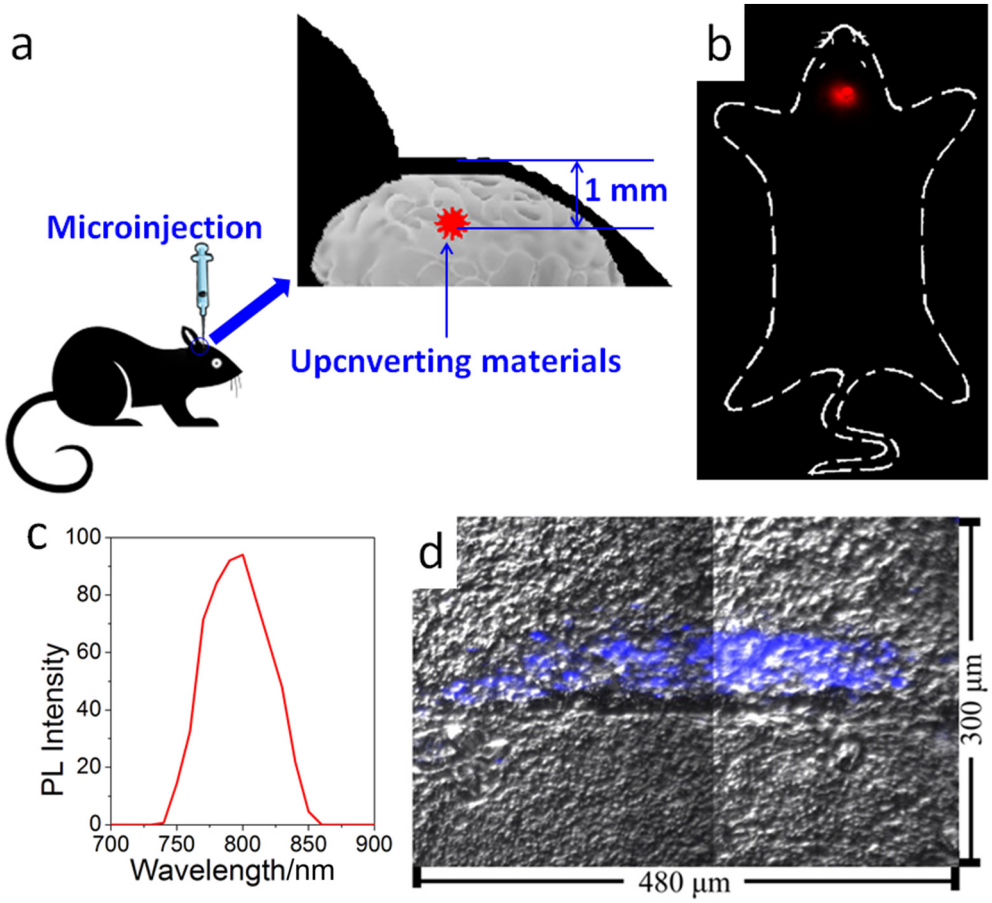

Fig. 10. (a) A diagram of microinjection of upconverting particles in a mouse brain; (b) *in vivo* upconversion luminescence imaging of mice injected with $NaYF_4$:Yb^{3+},Tm^{3+} microphosphors under excitation of 980 nm light; (c) spectra of the luminescence signal from the phosphors in mice brain observed in (b); (d) a typical upconversion luminescence image of the brain tissue slice from mice post-injected with $NaYF_4$:Yb^{3+},Tm^{3+} microphosphors for 2 weeks. The blue color revealed the distribution of the particles. Reproduced from Ref. [80] with permission from Elsevier.

and therapy is also an interesting topic. However, the cost performance for the design and synthesis of complex UCNPs based nanoplatform should be took into account at the early stage.

References

[1] D. Jaque, C. Richard, B. Viana, K. Soga, X. Liu, J. García Solé, Inorganic nanoparticles for optical bioimaging, *Adv. Opt. Photon.* 8 (1) (2016) 103.
[2] F. Cai, D. Wang, M. Zhu, S. He, Pencil-like imaging spectrometer for biosamples sensing, *Biomed. Opt. Express* 8 (2017) 5427–5436.
[3] J. Xie, G. Liu, H.S. Eden, H. Ai, X. Chen, Surface-engineered magnetic nanoparticle platforms for cancer imaging and therapy, *Acc. Chem. Res.* 44 (2011) 883–892.
[4] P.P. Laissue, R.A. Alghamdi, P. Tomancak, E.G. Reynaud, H. Shroff, Assessing phototoxicity in live fluorescence imaging, *Nat. Methods* 14 (2017) 657–661.
[5] D. Wang, Z. Wang, Q. Zhan, Y. Pu, J.-X. Wang, N.R. Foster, L. Dai, Facile and scalable preparation of fluorescent carbon dots for multifunctional applications, *Engineering* 3 (2017) 402–408.
[6] M.A. Miller, E. Kim, M.F. Cuccarese, A.L. Plotkin, M. Prytyskach, R.H. Kohler, M.J. Pittet, R. Weissleder, Near infrared imaging of Mer tyrosine kinase (MERTK) using MERi-SiR reveals tumor associated macrophage uptake in metastatic disease, *Chem. Commun.* 54 (2018) 42–45.
[7] Y. Wang, R. Hu, W. Xi, F. Cai, S. Wang, Z. Zhu, R. Bai, J. Qian, Red emissive AIE nanodots with high two-photon absorption efficiency at 1040 nm for deep-tissue *in vivo* imaging, *Biomed. Opt. Express* 6 (2015) 3783–3794.
[8] D. Wang, J.-F. Chen, L. Dai, Recent advances in graphene quantum dots for fluorescence bioimaging from cells through tissues to animals, *Part. Part. Syst. Charact.* 32 (2015) 515–523.
[9] D. Wang, L. Zhu, C. McCleese, C. Bruda, J.-F. Chen, L. Dai, Fluorescent carbon dots from milk by microwave cooking, *RSC Adv.* 6 (2016) 41516–41521.
[10] J.T. Hou, W.X. Ren, K. Li, J. Seo, A. Sharma, X.Q. Yu, J.S. Kim, Fluorescent bioimaging of pH: From design to applications, *Chem. Soc. Rev.* 46 (2017) 2076–2090.
[11] M.J. Schnermann, Chemical biology: Organic dyes for deep bioimaging, *Nature* 551 (2017) 176–177.
[12] J. Qian, B.Z. Tang, AIE Luminogens for bioimaging and theranostics: From organelles to animals, *Chem* 3 (2017) 56–91.
[13] X. Michalet, F.F. Pinaud, L.A. Bentolila, J.M. Tsay, S. Doose, J.J. Li, G. Sundaresan, A.M. Wu, S.S. Gambhir, S. Weiss, Quantum dots for live cells, *in vivo* imaging, and diagnostics, *Science* 307 (2005) 538–544.
[14] X. Gao, Y. Cui, R.M. Levenson, L.W.K. Chung, S. Nie, *In vivo* cancer targeting and imaging with semiconductor quantum dots, *Nat. Biotechnol.* 22 (2004) 969–976.
[15] X. Huang, J. Wu, Y. Zhu, Y. Zhang, X. Feng, X. Lu, Flow-resistance analysis of nano-confined fluids inspired from liquid nano-lubrication: A review, *Chin. J. Chem. Eng.* 25 (2017) 1552–1562.
[16] Y. Ji, W. Qian, Y. Yu, Q. An, L. Liu, Y. Zhou, C. Gao, Recent developments in nanofiltration membranes based on nanomaterials, *Chin. J. Chem. Eng.* 25 (2017) 1639–1652.
[17] A. Jayalakshmi, I.C. Kim, Y.N. Kwon, Suppression of gold nanoparticle agglomeration and its separation via nylon membranes, *Chin. J. Chem. Eng.* 25 (2017) 931–937.
[18] D. Wang, J. Qian, F. Cai, S. He, S. Han, Y. Mu, 'Green' synthesized near-infrared PbS quantum dots with silica-PEG dual-layer coating: Ultrastable and biocompatible optical probes for *in vivo* animal imaging, *Nanotechnology* 23 (2012), 245701.
[19] Y. Pu, F. Cai, D. Wang, J.-X. Wang, J.-F. Chen, Colloidal synthesis of semiconductor quantum dots toward large-scale production: A review, *Ind. Eng. Chem. Res.* 57 (2018) 1790–1802.
[20] D. Wang, J. Qian, W. Qin, A. Qin, B.Z. Tang, S. He, Biocompatible and photostable AIE dots with red emission for *in vivo* two-photon bioimaging, *Sci. Rep.* 4 (2014) 4279.
[21] T. Kao, F. Kohle, K. Ma, T. Aubert, A. Andrievsky, U. Wiesner, Fluorescent Silica Nanoparticles with well-separated intensity distributions from batch reactions, *Nano Lett.* 18 (2018) 1305–1310.
[22] W.M. Abdelwahab, E. Phillips, G. Patonay, Preparation of fluorescently labeled silica nanoparticles using an amino acid-catalyzed seeds regrowth technique: Application to latent fingerprints detection and hemocompatibility studies, *J. Colloid Interface Sci.* 512 (2018) 801–811.
[23] D. Wang, J. Liu, J.-F. Chen, L. Dai, Surface functionalization of carbon dots with polyhedraloligomericsilsesquioxane (POSS) for multifunctional applications, *Adv. Mater. Interfaces* 3 (2016), 1500439.
[24] J. Shen, S. Shang, X. Chen, D. Wang, Y. Cai, Highly fluorescent N, S-co-doped carbon dots and their potential applications as antioxidants and sensitive probes for Cr (VI) detection, *Sensors Actuators B Chem.* 248 (2017) 92–100.

Please cite this article as: Y. Pu, *et al.*, Recent progress in the green synthesis of rare-earth doped upconversion nanophosphors for optical bioimaging from cells to animals, *Chin. J. Chem. Eng.* (2017), https://doi.org/10.1016/j.cjche.2018.03.005

[25] J. Shen, S. Shang, X. Chen, D. Wang, Y. Cai, Facile synthesis of fluorescence carbon dots from sweet potato for Fe3 + sensing and cell imaging, *Mater. Sci. Eng. C* 76 (2017) 856–864.

[26] L. Li, Y. Liu, P. Hao, Z. Wang, L. Fu, Z. Ma, J. Zhou, PEDOT nanocomposites mediated dual-modal photodynamic and photothermal targeted sterilization in both NIR I and II window, *Biomaterials* 41 (2015) 132–140.

[27] D. Li, W. Qin, B. Xu, J. Qian, B.Z. Tang, AIE nanoparticles with high stimulated emission depletion efficiency and photobleaching resistance for long-term super-resolution bioimaging, *Adv. Mater.* 29 (2017), 1703643.

[28] N. Alifu, L. Yan, H. Zhang, A. Zebibula, Z. Zhu, W. Xi, A.W. Roe, B. Xu, W. Tian, J. Qian, Organic dye doped nanoparticles with NIR emission and biocompatibility for ultra-deep *in vivo* two-photon microscopy under 1040 nm femtosecond excitation, *Dyes Pigments* 143 (2017) 76–85.

[29] G. Chen, H. Qiu, P.N. Prasad, X. Chen, Upconversion nanoparticles: Design, nanochemistry, and applications in theranostics, *Chem. Rev.* 114 (2014) 5161–5214.

[30] D. Wang, L. Zhu, J.-F. Chen, L. Dai, Liquid marbles based on magnetic upconversion nanoparticles as magnetically and optically miniature reactors for photocatalysis and photodynamic therapy, *Angew. Chem. Int. Ed.* 55 (2016) 10795–10799.

[31] C. Yao, W. Wang, P. Wang, M. Zhao, X. Li, F. Zhang, Near-infrared upconversion mesoporous cerium oxide hollow biophotocatalyst for concurrent pH-/H_2O_2-responsive O_2-evolving synergetic cancer therapy, *Adv. Mater.* 30 (2018), 1704833.

[32] S. Chen, A.Z. Weitemier, X. Zeng, L. He, X. Wang, Y. Tao, A.J.Y. Huang, Y. Hashimotodani, M. Kano, H. Iwasaki, L.K. Parajuli, S. Okabe, D.B. Loong Teh, A.H. All, I. Tsutsui-Kimura, K.F. Tanaka, X. Liu, T.J. McHugh, Near-infrared deep brain stimulation *via* upconversion nanoparticle-mediated optogenetics, *Science* 359 (2018) 679–684.

[33] S. Hilderbrand, R. Weissleder, Near-infrared fluorescence: Application to *in vivo* molecular imaging, *Curr. Opin. Chem. Biol.* 14 (2010) 71–79.

[34] F. Cai, J. Yu, J. Qian, Y. Wang, Z. Chen, J. Huang, Z. Ye, S. He, Use of tunable second-harmonic signal from $KNbO_3$ nanoneedles to find optimal wavelength for deep-tissue imaging, *Laser Photonics Rev.* 8 (2015) 865–874.

[35] J. Qian, Z. Zhu, A. Qin, W. Qin, L. Chu, F. Cai, H. Zhang, Q. Wu, R. Hu, B.Z. Tang, S. He, High-order non-linear optical effects in organic luminogens with aggregation-induced emission, *Adv. Mater.* 27 (2015) 2332–2339.

[36] F. Wang, D. Banerjee, Y. Liu, X. Chen, X. Liu, Upconversion nanoparticles in biological labeling, imaging, and therapy, *Analyst* 135 (2010) 1839–1854.

[37] J. Zhou, Z. Liu, F. Li, Upconversion nanophosphors for small-animal imaging, *Chem. Soc. Rev.* 41 (2012) 1323–1349.

[38] O.S. Kwon, H.S. Song, J. Conde, H. Kim, N. Artzi, J.H. Kim, Dual-color emissive upconversion nanocapsules for differential cancer bioimaging *in vivo*, *ACS Nano* 10 (2016) 1512–1521.

[39] M.H. Alkahtani, F.S. Alghannam, C. Sanchez, C.L. Gomes, H. Liang, P.R. Hemmer, High efficiency upconversion nanophosphors for high-contrast bioimaging, *Nanotechnology* 27 (2016), 485501.

[40] M. Alkahtani, Y. Chen, J.J. Pedraza, J.M. González, D.Y. Parkinson, P.R. Hemmer, H. Liang, High resolution fluorescence bio-imaging upconversion nanoparticles in insects, *Opt. Express* 25 (2017) 1030–1039.

[41] X. Wen, B. Wang, R. Wu, N. Li, S. He, Q. Zhan, Yb^{3+}-enhanced UCNP@SiO_2 nanocomposites for consecutive imaging, photothermal-controlled drug delivery and cancer therapy, *Biomed, Opt. Express* 7 (2016) 2174–2185.

[42] J. Liu, R. Wu, N. Li, X. Zhang, Q. Zhan, S. He, Deep, high contrast microscopic cell imaging using three-photon luminescence of β-($NaYF_4$:Er^{3+}/$NaYF_4$) nanoprobe excited by 1480-nm CW laser of only 1.5-mW, *Biomed. Opt. Express* 6 (2015) 1857–1866.

[43] Y. Liu, Y. Lu, X. Yang, X. Zheng, S. Wen, F. Wang, X. Vidal, J. Zhao, D. Liu, Z. Zhou, Amplified stimulated emission in upconversion nanoparticles for super-resolution nanoscopy, *Nature* 543 (2017) 229–233.

[44] Q. Zhan, H. Liu, B. Wang, Q. Wu, R. Pu, C. Zhou, B. Huang, X. Peng, H. Ågren, S. He, Achieving high-efficiency emission depletion nanoscopy by employing cross relaxation in upconversion nanoparticles, *Nat. Commun.* 8 (2017) 1058.

[45] D. Wang, L. Zhu, Y. Pu, J.X. Wang, J.F. Chen, L. Dai, Transferrin-coated magnetic upconversion nanoparticles for efficient photodynamic therapy with near-infrared irradiation and luminescence bioimaging, *Nano* 9 (2017) 11214–11221.

[46] S. Li, S. Cui, D. Yin, Q. Zhu, Y. Ma, Z. Qian, Y. Gu, Dual antibacterial activities of a chitosan-modified upconversion photodynamic therapy system against drug-resistant bacteria in deep tissue, *Nano* 9 (2017) 3912–3924.

[47] S.S. Lucky, N.M. Idris, K. Huang, J. Kim, Z. Li, P.S. Thong, R. Xu, K.C. Soo, Y. Zhang, In vivo biocompatibility, biodistribution and therapeutic efficiency of titania coated upconversion nanoparticles for photodynamic therapy of solid oral cancers, *Theranostics* 6 (2016) 1844–1865.

[48] D. Wang, B. Liu, Z. Quan, C. Li, Z. Hou, B. Xing, J. Lin, New advances on the marrying of UCNPs and photothermal agents for imaging-guided diagnosis and the therapy of tumors, *J. Mater. Chem. B* 5 (2017) 2209–2230.

[49] X. Wu, Y. Zhang, K. Takle, O. Bilsel, Z. Li, H. Lee, Z. Zhang, D. Li, W. Fan, C. Duan, Dye-sensitized core/active shell upconversion nanoparticles for optogenetics and bioimaging applications, *ACS Nano* 10 (2016) 1060–1066.

[50] A. Bansal, H. Liu, M.K. Jayakumar, S. Andersson-Engels, Y. Zhang, Quasi-continuous wave near-infrared excitation of upconversion nanoparticles for optogenetic manipulation of C. elegans, *Small* 12 (2016) 1732–1743.

[51] A. Pliss, T.Y. Ohulchanskyy, G. Chen, J. Damasco, C.E. Bass, P.N. Prasad, Subcellular optogenetics enacted by targeted nanotransformers of near-infrared light, *ACS Photonics* 4 (2017) 806–814.

[52] K. Huang, Q. Dou, X.J. Loh, Nanomaterial mediated optogenetics: Opportunities and challenges, *RSC Adv.* 6 (2016) 60896–60906.

[53] X. Wang, R.R. Valiev, T.Y. Ohulchanskyy, Å. H, C. Yang, G. Chen, Dye-sensitized lanthanide-doped upconversion nanoparticles, *Chem. Soc. Rev.* 46 (2017) 4150–4167.

[54] G. Chen, H. Agren, T.Y. Ohulchanskyy, P.N. Prasad, Light upconverting core-shell nanostructures: Nanophotonic control for emerging applications, *Chem. Soc. Rev.* 44 (2015) 1680–1713.

[55] A. Sedlmeier, D.E. Achatz, L.H. Fischer, H.H. Gorris, O.S. Wolfbeis, Photon upconverting nanoparticles for luminescent sensing of temperature, *Nano* 4 (2012) 7090–7096.

[56] X. Chen, D. Peng, Q. Ju, F. Wang, Photon upconversion in core-shell nanoparticles, *Chem. Soc. Rev.* 44 (2015) 1318–1330.

[57] J. Hesse, D.T. Klier, M. Sgarzi, A. Nsubuga, C. Bauer, J. Grenzer, R. Hübner, M. Wislicenus, T. Joshi, M.U. Kumke, H. Stephan, *Chem. Open* 7 (2018) 159–168.

[58] X. Liu, C.-H. Yan, J.A. Capobianco, Photon upconversion nanomaterials, *Chem. Soc. Rev.* 44 (2015) 1299–1301.

[59] D. Yang, P. Ma, Z. Hou, Z. Cheng, C. Li, J. Lin, Current advances in lanthanide ion (Ln^{3+})-based upconversion nanomaterials for drug delivery, *Chem. Soc. Rev.* 44 (2015) 1416–1448.

[60] D. Chen, P. Huang, Y. Yu, F. Huang, A. Yang, Y. Wang, Dopant-induced phase transition: A new strategy of synthesizing hexagonal upconversion $NaYF_4$ at low temperature, *Chem. Commun.* 47 (2011) 5801–5803.

[61] Q. Zhan, J. Qian, H. Liang, G. Somesfalean, D. Wang, S. He, Z. Zhang, S.A. Engels, Using 915 nm laser excited Tm^{3+}/Er^{3+}/Ho^{3+}-doped $NaYbF_4$ upconversion nanoparticles for *in vitro* and deeper *in vivo* bioimaging without overheating irradiation, *ACS Nano* 5 (2011) 3744–3757.

[62] T. Rinkel, A.N. Raj, S. Dühnen, M. Haase, Synthesis of 10 nm β-$NaYF_4$:Yb,Er/$NaYF_4$ Core/Shell upconversion nanocrystals with 5 nm particle cores, *Angew. Chem. Int. Ed.* 55 (2016) 1164–1167.

[63] P. Lei, R. An, S. Yao, Q. Wang, L. Dong, X. Xu, K. Du, J. Feng, H. Zhang, Ultrafast synthesis of novel hexagonal phase $NaBiF_4$ upconversion nanoparticles at room temperature, *Adv. Mater.* 29 (2017), 1700505.

[64] Y. Feng, H. Chen, L. Ma, B. Shao, S. Zhao, Z. Wang, H. You, Surfactant-free aqueous synthesis of novel Ba_2GdF_7:Yb^{3+},Er^{3+}@PEG upconversion nanoparticles for *in vivo* trimodality imaging, *ACS Appl. Mater. Interfaces* 9 (2017) 15096–15102.

[65] J. Zhou, Q. Liu, W. Feng, Y. Sun, F. Li, Upconversion luminescent materials: Advances and applications, *Chem. Rev.* 115 (2015) 395–465.

[66] M. Longmire, P.L. Choyke, H. Kobayashi, Clearance properties of nano-sized particles and molecules as imaging agents: Considerations and caveats, *Nanomedicine* 3 (2008) 703–717.

[67] J. Qian, L. Jiang, F. Cai, D. Wang, S. He, Fluorescence-surface enhanced Raman scattering co-functionalized gold nanorods as near-infrared probes for purely optical *in vivo* imaging, *Biomaterials* 32 (2011) 1602–1610.

[68] J.P. Zimmer, S.W. Kim, S. Ohnishi, E. Tanaka, J.V. Frangioni, M.G. Bawendi, Size series of small indium arsenide-zinc selenide core-shell nanocrystals and their application to *in vivo* imaging, *J. Am. Chem. Soc.* 128 (2006) 2526–2527.

[69] G.S. Yi, G.M. Chow, Water-soluble $NaYF_4$:Yb,Er(Tm)/$NaYF_4$/polymer core/shell/shell nanoparticles with significant enhancement of upconversion fluorescence, *Chem. Mater.* 19 (2007) 341–343.

[70] J. Shen, G. Chen, T.Y. Ohulchanskyy, S.J. Kesseli, S. Buchholz, Z. Li, P.N. Prasad, G. Han, Tunable near infrared to ultraviolet upconversion luminescence enhancement in (α-$NaYF_4$:Yb,Tm)/CaF_2 core/shell nanoparticles for *in situ* real-time recorded biocompatible photoactivation, *Small* 9 (2013) 3213–3217.

[71] G. Chen, W. Shao, R.R. Valiev, T.Y. Ohulchanskyy, G.S. He, H. Ågren, P.N. Prasad, Efficient broadband upconversion of near-infrared light in dye-sensitized core/shell nanocrystals, *Adv. Opt. Mater.* 4 (2016) 1760–1766.

[72] W. Zou, C. Visser, J.A. Maduro, M.S. Pshenichnikov, J.C. Hummelen, Broadband dye-sensitized upconversion of near-infrared light, *Nat. Photonics* 6 (2012) 560–564.

[73] G. Chen, J. Damasco, H. Qiu, S. Wei, T.Y. Ohulchanskyy, R.R. Valiev, X. Wu, G. Han, Y. Wang, C. Yang, P.N. Prasad, H. Ågren, Energy-cascaded upconversion in an organic dye-sensitized core/shell fluoride nanocrystal, *Nano Lett.* 15 (2015) 7400–7407.

[74] H. Kobayashi, M. Ogawa, R. Alford, P.L. Choyke, Y. Urano, New strategies for fluorescent probe design in medical diagnostic imaging, *Chem. Rev.* 110 (2010) 2620–2640.

[75] J.C. Goldschmidt, S. Fischer, Upconversion for photovoltaics-a review of materials, devices and concepts for performance enhancement, *Adv. Opt. Mater.* 3 (2015) 510–535.

[76] M.V. Dacosta, S. Doughan, Y. Han, U.J. Krull, Lanthanide upconversion nanoparticles and applications in bioassays and bioimaging: A review, *Anal. Chim. Acta* 832 (2014) 1–33.

[77] B. Zhou, B. Shi, D. Jin, X. Liu, Controlling upconversion nanocrystals for emerging applications, *Nat. Nanotechnol.* 10 (2015) 924–936.

[78] J. Shan, Y. Ju, A single-step synthesis and the kinetic mechanism for monodisperse and hexagonal-phase $NaYF_4$:Yb,Er upconversion nanophosphors, *Nanotechnology* 20 (2009), 275603.

[79] P. Huang, W. Zheng, S. Zhou, D. Tu, Z. Chen, H. Zhu, R. Li, E. Ma, M. Huang, X. Chen, Lanthanide-doped $LiLuF_4$ upconversion nanoprobes for the detection of disease biomarkers, *Angew. Chem. Int. Ed.* 53 (2014) 1252–1257.

[80] Y. Pu, L. Lin, D. Wang, J.X. Wang, J. Qian, J.F. Chen, Green synthesis of highly dispersed ytterbium and thulium co-doped sodium yttrium fluoride microphosphors for *in situ* light upconversion from near-infrared to blue in animals, *J. Colloid Interface Sci.* 511 (2018) 243–250.

[81] Y.Q. Zhang, D. Wang, L.L. Zhang, Y. Le, J.X. Wang, J.F. Chen, Facile preparation of α-calcium sulfate hemihydrate with low aspect ratio using high-gravity reactive precipitation combined with salt solution method at atmospheric pressure, *Ind. Eng. Chem. Res.* 56 (2017) 14053–14059.

Please cite this article as: Y. Pu, *et al.*, Recent progress in the green synthesis of rare-earth doped upconversion nanophosphors for optical bioimaging from cells to animals, *Chin. J. Chem. Eng.* (2017), https://doi.org/10.1016/j.cjche.2018.03.005

[82] F. Kang, D. Wang, Y. Pu, X.F. Zeng, J.X. Wang, J.F. Chen, Efficient preparation of monodisperse $CaCO_3$ nanoparticles as overbased nanodetergents in a high-gravity rotating packed bed reactor, *Powder Technol.* 325 (2018) 405–411.
[83] X. Yang, J. Leng, D. Wang, Z. Wang, J.-X. Wang, Y. Pu, J. Shui, J.-F. Chen, Synthesis of flower-shaped V_2O_5:Fe^{3+} microarchitectures in a high-gravity rotating packed bed with enhanced electrochemical performance for lithium ion batteries, *Chem. Eng. Process.* 120 (2017) 201–206.
[84] K.L. Reddy, N. Prabhakar, R. Arppe, J.M. Rosenholm, V. Krishnan, Microwave-assisted one-step synthesis of acetate-capped $NaYF_4$:Yb/Er upconversion nanocrystals and their application in bioimaging, *J. Mater. Sci.* 52 (2017) 5738–5750.
[85] G. Yi, H. Lu, S. Zhao, Y. Ge, W. Yang, D. Chen, L.H. Guo, Synthesis, characterization, and biological application of size-controlled nanocrystalline $NaYF_4$:Yb,Er infrared-to-visible up-conversion phosphors, *Nano Lett.* 4 (2004) 2191–2196.
[86] Y. Tian, B. Tian, P. Huang, L. Wang, B. Chen, Size-dependent upconversion luminescence and temperature sensing behavior of spherical Gd_2O_3:Yb^{3+}/Er^{3+} phosphor, *RSC Adv.* 5 (2015) 14123–14128.
[87] S. Shah, J.J. Liu, N. Pasquale, J. Lai, H. McGowan, Z.P. Pang, K.B. Lee, Hybrid upconversion nanomaterials for optogenetic neuronal control, *Nano* 7 (2015) 16571–16577.
[88] H. Shang, X. Zhang, J. Xu, Y. Han, Effects of preparation methods on the activity of CuO/CeO_2 catalysts for CO oxidation, *Front. Chem. Sci. Eng.* 11 (2017) 603–612.
[89] Z. Mao, C. Yang, Micro-mixing in chemical reactors: A perspective, *Chin. J. Chem. Eng.* 25 (2017) 381–390.
[90] G.W. Chu, Y.J. Song, W.J. Zhang, Y. Luo, H.K. Zou, Y. Xiang, J.F. Chen, Micromixing efficiency enhancement in a rotating packed bed reactor with surface-modified nickel foam packing, *Ind. Eng. Chem. Res.* 54 (2015) 1697–1702.
[91] J. Leng, J. Chen, D. Wang, J.-X. Wang, Y. Pu, J.-F. Chen, Scalable preparation of Gd_2O_3:Yb^{3+}/Er^{3+} upconversion nanophosphors in a high-gravity rotating packed bed reactor for transparent upconversion luminescent films, *Ind. Eng. Chem. Res.* 56 (2017) 7977–7983.
[92] Y. Yang, Y. Sun, T. Cao, J. Peng, Y. Liu, Y. Wu, W. Feng, Y. Zhang, F. Li, Hydrothermal synthesis of $NaLuF_4$:^{153}Sm,Yb,Tm nanoparticles and their application in dual-modality upconversion luminescence and SPECT bioimaging, *Biomaterials* 34 (2013) 774–783.
[93] P. Du, P. Zhang, S.H. Kang, J.S. Yu, Hydrothermal synthesis and application of Ho^{3+}-activated $NaYbF^4$ bifunctional upconverting nanoparticles for *in vitro* cell imaging and latent fingerprint detection, *Sensors Actuators B Chem.* 252 (2017) 584–591.
[94] K.L. Reddy, M. Rai, N. Prabhakar, R. Arppe, S.B. Rai, S.K. Singh, J.M. Rosenholm, V. Krishnan, Controlled synthesis, bioimaging and toxicity assessments in strong red emitting Mn^{2+} doped $NaYF_4$:Yb^{3+}/Ho^{3+} nanophosphors, *RSC Adv.* 6 (2016) 53698–53704.
[95] X. Wang, J. Zhuang, Q. Peng, Y. Li, A general strategy for nanocrystal synthesis, *Nature* 437 (2005) 121–124.
[96] L. Zhou, Z. Li, Z. Liu, M. Yin, J. Ren, X. Qu, One-step nucleotide-programmed growth of porous upconversion nanoparticles: Application to cell labeling and drug delivery, *Nano* 6 (2014) 1445–1452.
[97] P. Qiu, N. Zhou, Y. Wang, C. Zhang, Q. Wang, R. Sun, G. Gao, D. Cui, Tuning lanthanide ion-doped upconversion nanocrystals with different shapes *via* a one-pot cationic surfactant-assisted hydrothermal strategy, *CrystEngComm* 16 (2014) 1859–1863.
[98] R. Sun, P. Qiu, T. Yin, G. Gao, H. Fu, K. Wang, C. Zhang, Potassium sodium tartrate-assisted hydrothermal synthesis of $BaLuF_5$:Yb^{3+}/Er^{3+} nanocrystals, *Particuology* 24 (2015) 164–169.
[99] S.L. Pirard, S. Douven, J.P. Pirard, Large-scale industrial manufacturing of carbon nanotubes in a continuous inclined mobile-bed rotating reactor via the catalytic chemical vapor deposition process, *Front. Chem. Sci. Eng.* 11 (2017) 280–289.
[100] P.K. Fard, E. Afshari, M.Z. Rad, S.T. Dehaghani, A numerical study on heat transfer enhancement and design of a heat exchanger with porous media in continuous hydrothermal flow synthesis system, *Chin. J. Chem. Eng.* 25 (2017) 1352–1359.
[101] L. Zhang, S. Wu, Z. Liang, H. Zhao, H. Zou, G. Chu, Hydrogen sulfide removal by catalytic oxidative absorption method using rotating packed bed reactor, *Chin. J. Chem. Eng.* 25 (2017) 175–179.
[102] H.Y. Shen, Y.Z. Liu, *In situ* synthesis of hydrophobic magnesium hydroxide nanoparticles in a novel impinging stream-rotating packed bed reactor, *Chin. J. Chem. Eng.* 24 (2016) 1306–1312.
[103] S. Mortazavi, Computational analysis of the flow of pseudoplastic power-law fluids in a microchannel plate, *Chin. J. Chem. Eng.* 25 (2017) 1360–1368.
[104] M. Akbari, M. Rahimi, M. Faryadi, Gas–liquid flow mass transfer in a T-shape microreactor stimulated with 1.7 MHz ultrasound waves, *Chin. J. Chem. Eng.* 25 (2017) 1143–1152.
[105] K. Huanbutta, P. Sriamornsak, M. Luangtana-Anan, S. Limmatvapirat, S. Puttipipatkhachorn, L.Y. Lim, K. Terada, J. Nunthanid, Application of multiple step-wise spinning disk processing for the synthesis of poly(methyl acrylates) coated chitosan–diclofenac sodium nanoparticles for colonic drug delivery, *Eur. J. Pharm. Sci.* 50 (2013) 303–311.
[106] J. Liu, W. Bu, L. Pan, J. Shi, NIR-triggered anticancer drug delivery by upconverting nanoparticles with integrated azobenzene-modified mesoporous silica, *Angew. Chem. Int. Ed.* 52 (2013) 4375–4379.
[107] Y. Liu, W. Hou, H. Sun, C. Cui, L. Zhang, Y. Jiang, Y. Wu, Y. Wang, J. Li, B.S. Sumerlin, Q. Liu, W. Tan, Thiol-ene click chemistry: A biocompatible way for orthogonal bioconjugation of colloidal nanoparticles, *Chem. Sci.* 8 (2017) 6182–6187.
[108] W. Kong, T. Sun, B. Chen, X. Chen, F. Ai, X. Zhu, M. Li, W. Zhang, G. Zhu, F. Wang, A general strategy for ligand exchange on upconversion nanoparticles, *Inorg. Chem.* 56 (2017) 872–877.
[109] Z. Chen, H. Chen, H. He, M. Yu, F. Li, Z. Qiang, Z. Zhou, T. Yi, C. Huang, Versatile synthesis strategy for carboxylic acid — functionalized upconverting nanophosphors as biological labels, *J. Am. Chem. Soc.* 130 (2008) 3023–3029.
[110] G.K. Das, D.T. Stark, I.M. Kennedy, Potential toxicity of up-converting nanoparticles encapsulated with a bilayer formed by ligand attraction, *Langmuir* 30 (2014) 8167–8176.
[111] X. Li, D. Shen, J. Yang, C. Yao, R. Che, F. Zhang, D. Zhao, Successive layer-by-layer strategy for multi-shell epitaxial growth: Shell thickness and doping position dependence in upconverting optical properties, *Chem. Mater.* 25 (2013) 106–112.
[112] J. Shen, K. Li, L. Cheng, Z. Liu, S.T. Lee, J. Liu, Specific detection and simultaneously localized photothermal treatment of cancer cells using layer-by-layer assembled multifunctional nanoparticles, *ACS Appl. Mater. Interfaces* 6 (2014) 6443–6452.
[113] A. Escudero, C. Carrillo-Carrión, M.V. Zyuzin, W.J. Parak, Luminescent rare-earth-based nanoparticles: A summarized overview of their synthesis, functionalization, and applications, *Top. Curr. Chem.* 374 (2016) 48.
[114] W.F. Lai, A.L. Rogach, W.T. Wong, Molecular design of upconversion nanoparticles for gene delivery, *Chem. Sci.* 8 (2017) 7339–7358.
[115] C.T. Xu, Q. Zhan, H. Liu, G. Somesfalean, J. Qian, S. He, S. Andersson-Engels, Upconverting nanoparticles for pre-clinical diffuse optical imaging, microscopy and sensing: Current trends and future challenges, *Laser Photonics Rev.* 7 (2013) (2013) 663–697.
[116] W. Zheng, S. Zhou, Z. Chen, P. Hu, Y. Liu, D. Tu, H. Zhu, R. Li, M. Huang, X. Chen, Sub-10 nm lanthanide-doped CaF_2 nanoprobes for time-resolved luminescent biodetection, *Angew. Chem. Int. Ed.* 52 (2013) 6671–6676.
[117] Q. Liu, W. Feng, T. Yang, T. Yi, F. Li, Upconversion luminescence imaging of cells and small animals, *Nat. Protoc.* 8 (2013) 2033–2044.
[118] H.J. Zijlmans, J. Bonnet, J. Burton, K. Kardos, T. Vail, R.S. Niedbala, H.J. Tanke, Detection of cell and tissue surface antigens using up-converting phosphors: A new reporter technology, *Anal. Biochem.* 267 (1999) 30–36.
[119] C. Wang, L. Cheng, Z. Liu, Drug delivery with upconversion nanoparticles for multi-functional targeted cancer cell imaging and therapy, *Biomaterials* 32 (2011) 1110–1120.
[120] P.Y. Yuan, Y.H. Lee, M.K. Gnanasammandhan, Z. Guan, Y. Zhang, Q.H. Xu, Plasmon enhanced upconversion luminescence of $NaYF_4$:Yb,Er@SiO_2@Ag core-shell nanocomposites for cell imaging, *Nano* 4 (2012) 5132–5137.
[121] M. Yu, F. Li, Z. Chen, H. Hu, C. Zhan, H. Yang, C. Huang, Laser scanning upconversion luminescence microscopy for imaging cells labeled with rare-earth nanophosphors, *Anal. Chem.* 81 (2009) 930–935.
[122] Q. Zhan, S. He, J. Qian, C. Hao, F. Cai, Optimization of optical excitation of upconversion nanoparticles for rapid microscopy and deeper tissue imaging with higher quantum yield, *Theranostics* 3 (2013) 306–316.
[123] Y.F. Wang, G.Y. Liu, L.D. Sun, J.W. Xiao, J.C. Zhou, C.H. Yan, Nd^{3+}-sensitized upconversion nanophosphors: Efficient in vivo bioimaging probes with minimized heating effect, *ACS Nano* 7 (2013) 7200–7206.
[124] Y. Zhong, G. Tian, Z. Gu, Y. Yang, L. Gu, Y. Zhao, Y. Ma, J. Yao, Elimination of photon quenching by a transition layer to fabricate a quenching-shield sandwich structure for 800 nm excited upconversion luminescence of Nd^{3+}-sensitized nanoparticles, *Adv. Mater.* 26 (2014) 2831–2837.
[125] Q. Wu, B. Huang, X. Peng, S. He, Q. Zhan, Non-bleaching fluorescence emission difference microscopy using single 808-nm laser excited red upconversion emission, *Opt. Express* 25 (2017) 30885–30894.
[126] R. Kolesov, R. Reuter, K. Xia, R. Stöhr, A. Zappe, J. Wrachtrup, Super-resolution upconversion microscopy of praseodymium-doped yttrium aluminum garnet nanoparticles, *Phys. Rev. B* 84 (2011) (2011) 153413.
[127] R. Wu, Q. Zhan, H. Liu, X. Wen, B. Wang, S. He, Optical depletion mechanism of upconverting luminescence and its potential for multi-photon STED-like microscopy, *Opt. Express* 23 (2015) 2401–32412.
[128] M. Nyk, R. Kumar, T.Y. Ohulchanskyy, E.J. Bergey, P.N. Prasad, High contrast in vitro and in vivo photoluminescence bioimaging using near infrared to near infrared upconversion in Tm^{3+} and Yb^{3+} doped fluoride nanophosphors, *Nano Lett.* 8 (2008) 3834–3838.
[129] Q. Liu, M. Xu, T. Yang, B. Tian, X. Zhang, F. Li, Highly photostable near-IR-excitation upconversion nanocapsules based on triplet-triplet annihilation for *in vivo* bioimaging application, *ACS Appl. Mater. Interfaces* 10 (2018) 9883–9888.
[130] C. Duan, L. Liang, L. Li, R. Zhang, Z.P. Xu, Recent progress in upconversion luminescence nanomaterials for biomedical applications, *J. Mater. Chem. B* 6 (2018) 192–209.
[131] J. Rieffel, F. Chen, J. Kim, G. Chen, W. Shao, S. Shao, U. Chitgupi, R. Hernandez, S.A. Graves, R.J. Nickles, Hexamodal imaging with porphyrin-phospholipid-coated upconversion nanoparticles, *Adv. Mater.* 27 (2015) 1785–1790.
[132] S.A. Hilderbrand, F. Shao, C. Salthouse, U. Mahmood, R. Weissleder, Upconverting luminescent nanomaterials: Application to *in vivo* bioimaging, *Chem. Commun.* (28) (2009) 4188–4190.
[133] N.M. Idris, Z. Li, L. Ye, E.K.W. Sim, R. Mahendran, P.C.L. Ho, Y. Zhang, Tracking transplanted cells in live animal using upconversion fluorescent nanoparticles, *Biomaterials* 30 (2009) 5104–5113.
[134] L. Pan, M. He, J. Ma, W. Tang, G. Gao, R. He, H. Su, D. Cui, Phase and size controllable synthesis of $NaYbF_4$ nanocrystals in oleic acid/ionic liquid two-phase system for targeted fluorescent imaging of gastric cancer, *Theranostics* 3 (2013) 210–222.
[135] J. Zhou, Y. Sun, X. Du, L. Xiong, H. Hua, F. Li, Dual-modality *in vivo* imaging using rare-earth nanocrystals with near-infrared to near-infrared (NIR-to-NIR) upconversion luminescence and magnetic resonance properties, *Biomaterials* 31 (2010) 3287–3295.

Please cite this article as: Y. Pu, *et al.*, Recent progress in the green synthesis of rare-earth doped upconversion nanophosphors for optical bioimaging from cells to animals, *Chin. J. Chem. Eng.* (2017), https://doi.org/10.1016/j.cjche.2018.03.005

[136] J.-C. Boyer, M.-P. Manseau, J.I. Murray, F.C.J.M. van Veggel, Surface modification of upconverting $NaYF_4$ nanoparticles with PEG-phosphate ligands for NIR (800 nm) biolabeling within the biological window, *Langmuir* 26 (2010) 1157–1164.

[137] T. Yang, Y. Sun, Q. Liu, W. Feng, P. Yang, F. Li, Cubic sub-20 nm $NaLuF_4$-based upconversion nanophosphors for high-contrast bioimaging in different animal species, *Biomaterials* 33 (2012) 3733–3742.

[138] X. Ge, L. Dong, L. Sun, Z. Song, R. Wei, L. Shi, H. Chen, New nanoplatforms based on UCNPs linking with polyhedral oligomeric silsesquioxane (POSS) for multimodal bioimaging, *Nano* 7 (2015) 7206–7215.

[139] D. Ni, W. Bu, S. Zhang, X. Zheng, M. Li, H. Xing, Q. Xiao, Y. Liu, Y. Hua, L. Zhou, W. Peng, K. Zhao, J. Shi, Single Ho^{3+}-doped upconversion nanoparticles for high-performance T_2-weighted brain tumor diagnosis and MR/UCL/CT multimodal imaging, *Adv. Funct. Mater.* 24 (2014) 6613–6620.

[140] J. Rieffel, U. Chitgupi, J.F. Lovell, Recent advances in higher-order, multimodal, biomedical imaging agents, *Small* 11 (2015) 4445–4461.

[141] S. Sundaramoorthy, A. Garcia Badaracco, S.M. Hirsch, J.H. Park, T. Davies, J. Dumont, M. Shirasu-Hiza, A.C. Kummel, J.C. Canman, Low efficiency upconversion nanoparticles for high-resolution coalignment of near-infrared and visible light paths on a light microscope, *ACS Appl. Mater. Interfaces* 9 (2017) 7929–7940.

[142] Y. Wang, X. Lin, X. Chen, X. Chen, Z. Xu, W. Zhang, Q. Liao, X. Duan, X. Wang, M. Liu, F. Wang, J. He, P. Shi, Tetherless near-infrared control of brain activity in behaving animals using fully implantable upconversion microdevices, *Biomaterials* 142 (2017) 136–148.

[143] Y. Sun, W. Feng, P. Yang, C. Huang, F. Li, The biosafety of lanthanide upconversion nanomaterials, *Chem. Soc. Rev.* 44 (2015) 1509–1525.

Please cite this article as: Y. Pu, *et al.*, Recent progress in the green synthesis of rare-earth doped upconversion nanophosphors for optical bioimaging from cells to animals, *Chin. J. Chem. Eng.* (2017), https://doi.org/10.1016/j.cjche.2018.03.005